CHAPTER-1

INTRODUCTION

1.1 Power System Stability

Power system stability is the ability of an electric power system, for a given initial operating condition, to regain a state of operating equilibrium after being subjected to a physical disturbance, with most of the system variables bounded so that practically the entire system remains intact. The disturbances could be faults, load changes, generator outages, line outages, voltage collapse or some combination of these. Power system stability can be broadly classified into rotor angle, voltage, and frequency stability. Each of these three stabilities can be further classified into large disturbance or small disturbance, short term or long term.

Rotor angle stability is the ability of the system to remain in synchronism when subjected to a disturbance. The rotor angle of a generator depends on the balance between the electromagnetic torque due to the generator electrical power output and mechanical torque due to the input mechanical power through a prime mover. Remaining in synchronism means that all the generators electromagnetic torque is exactly balanced by the mechanical torque. If in some generator the balance between electromagnetic and mechanical torque is disturbed, due to disturbances in the system, then this will lead to oscillations in the rotor angle.

Voltage stability is the ability of the system to maintain steady state voltages at all the system buses when subjected to a disturbance. If the disturbance is large then it is called as large-disturbance voltage stability and if the disturbance is small it is called as small-disturbance voltage stability. Unlike angle stability, voltage stability can also be a long term phenomenon. In case voltage fluctuations occur due to fast acting devices like induction motors, power electronic drive, HVDC etc then the time frame for understanding the stability is in the range of 10-20 s and hence can be treated as short term phenomenon. On the other hand if voltage variations are due to slow change in load, over loading of lines, generators hitting reactive power limits.

Frequency stability refers to the ability of a power system to maintain steady frequency following a severe disturbance between generation and load. It depends on the ability to restore equilibrium between system generation and load, with minimum loss of load. Frequency instability

may lead to sustained frequency swings leading to tripping of generating units or loads. During frequency excursions, the characteristic times of the processes and devices that are activated will range from fraction of seconds like under frequency control to several minutes, corresponding to the response of devices such as prime mover and hence frequency stability may be a short-term phenomenon or a long-term phenomenon.

Though, stability is classified into rotor angle, voltage and frequency stability they need not be independent isolated events. A voltage collapse at a bus can lead to large excursions in rotor angle and frequency. Similarly, large frequency deviations can lead to large changes in voltage magnitude.

1.1.1 Power System Oscillation

The electro-mechanical coupling between the synchronous machines rotor and the rest of the system exhibits low frequency oscillatory behavior following any disturbance from the equilibrium state. Such disturbances are due to minor variations in load and generations. These small signal oscillations with low frequency often persist for long periods of time and in some cases they even cause limitations on power transfer capability. A power system having several such machines will exhibit multiple modes of oscillation. These power swing modes usually occur in the frequency range of 0.2 to 3.0 Hz.

Electromechanical oscillation can be classified in five main categories, namely:

- Intra-plant mode oscillations
- Local plant mode oscillations
- Inter-area mode oscillations
- Control mode oscillations
- Torsional modes between rotating plant

Intra-plant Mode Oscillation**:** Machines on the same power generation site oscillate against each other at 2.0 to 3.0 Hz depending on the unit ratings and the reactance connecting them. This oscillation is termed as intra-plant because the oscillations manifest themselves within the generation plant complex. The rest of the system is unaffected.

Local plant Mode Oscillations: In local mode, one generator swings against the rest of the system at 1.0 to 2.0 Hz. The impact of the oscillation is localized to the generator and the line connecting it to the grid.

Inter-area Mode Oscillations: This phenomenon is observed over a large part of the network. It involves two coherent group groups of generators swinging against each other at 1 Hz or less. The oscillation frequency is approximately 0.3 Hz. This complex phenomenon involves many parts of the system with highly non-linear dynamic behavior.

Control Mode Oscillations: These are associated with generators and poorly tuned exciters, governors, HVDC converters and SVC controls. Loads and excitation systems can interact through control modes.

Torsional Modes Oscillation between Rotating Plant: These modes are associated with a turbine generator shaft system in the frequency range of 10-46 Hz .Usually these modes are excited when a multi-stage turbine generator is connected to the grid system through a series compensated line. A mechanical torsional mode of the shaft system interacts with the series capacitor at the natural frequency of the electrical network.

1.1.2 Low Frequency Oscillations

Low frequency oscillations (LFOs) are generator rotor angle oscillations having a frequency between 0.1 Hz to 3.0 Hz and are defined by how they are created or where they are located in the power system. The mitigation of these oscillations is commonly performed with supplementary stabilizing signals and the networks used to generate these signals have come to be known as power system stabilizer networks. LFOs include local plant modes, control modes, torsional modes induced by the interaction between the mechanical and electrical modes of a turbine-generator system, and inter- area modes, which may be caused by either high gain exciters or heavy power transfers across weak tie lines.

Low frequency oscillations can be created by small disturbances in the system, such as changes in the load and are normally analyzed through the small-signal stability (linear response) of the power system. These small disturbances lead to a steady increase or decrease in generator rotor

angle caused by the lack of synchronizing torque, or to rotor oscillations of increasing amplitude due to a lack of sufficient damping torque. The most typical instability is the lack of a sufficient damping torque on the rotor's low frequency oscillations.

Power swing modes have very little inherent damping. Damping is usually due to steam or water flow against the turbine blades of generating units and due to damper winding present in the rotor surface of the generators .High power flow in transmission system creates conditions where swing modes experience destabilization. The effect of oscillations on the power system may be disruptive if they become too large or are under damped. They can result in voltage oscillation in the power system, adversely affecting the system's performance. Additionally, limitation may be imposed on the power transfer between areas to reduce the possibility of sustained or growing oscillations, or special control may be added to damp this oscillation.

1.1.3 Conventional Power System Stabilizers (CPSS)

Some of the earliest power system stability problems included spontaneous power system oscillations at low frequencies. These low frequency oscillations (LFOs) are related to the small signal stability of a power system and are detrimental to the goals of maximum power transfer and power system security.

Power System Stabilizers are used to generate supplementary control signals for the excitation system in order to damp oscillation. The basic function of PSS is to extend the stability limit by modulating generator excitation to provide positive damping torque to powers wing modes.

A typical PSS consists of a phase compensation stage, a signal washout stage, and a gain block. To provide damping, a PSS must provide a component of electrical torque on the rotor in phase with the speed deviations. The implementation details differ, depending on the stabilizer input signal employed. PSS input signals which have been used including generator speed, frequency, and power. For any input signal, the transfer function of the PSS must compensate for the gain and phase characteristics of the excitation system, the generator, and the power system. These collectively determine the transfer function from the stabilizer output to the component of electrical torque which can be modulated via excitation control.

The PSS, while damping the rotor oscillations, can cause instability of the turbine generator shaft torsional modes. Selection of shaft speed pick-up location and torsional notch filters are used to attenuate the torsional mode frequency signals. The PSS gain and torsional filters however, adversely affects the exciter mode damping ratio. The use of accelerating power as input signal for the PSS, attenuates the shaft torsional modes inherently and mitigate the requirements of the filtering in the main stabilizing path.

The conventional power system stabilizer such as lead-lag, proportional integral (PI) power system stabilizer, proportional integral derivative (PID) power system stabilizer are tuned to operate at a particular operating condition. So, the disadvantage of this type of stabilizer is that they cannot operate under different disturbances. This limitation of conventional PSS can be overcome by a PSS design based on intelligence techniques viz. fuzzy logic technique, neural network, genetic algorithm etc.

1.1.4 Fuzzy Power System Stabilizers (FPSS)

The conventional power system stabilizers suffer from a limitation that these are not much efficient for damping small signal oscillations over wide range of operating conditions. It requires a deep understanding of a system, its exact equations and precise numeric values. To overcome these problems a fuzzy power system stabilizer has been developed using the concept of fuzzy basis functions. The linguistic rules, regarding the dependence of the plant output on the controlling signal are used to build the Fuzzy Power System Stabilizer. Limitation of fixed parameter of conventional PSS has been overcome in Fuzzy logic control PSS. For steady state operation, the system with fuzzy logic PSS settles down much faster than system with conventional PSS.

1.2 Literature Survey

A. Dysko, W.E. Leithead and J. O'Reilly [1] have described a step-by-step coordinated design procedure for power system stabilizers (PSSs) and automatic voltage regulators (AVRs) in a strongly coupled system. The proposed coordinated PSS/AVR design procedure is established within a frequency- domain framework. G Guralla, R Padhi and I Sen [2] have proposed a method of designing fixed parameter decentralized power system stabilizers (PSS) for interconnected multi machine power systems. Here Heffron - Philips model is used to decide the structure of the

PSS compensator and tune its parameters at each machine in the multi machine environment. A. Chatterjee, S.P. Ghosal, and V. Mukherjee [3] have described a comparative transient performance of single-input conventional power system stabilizer (CPSS) and dual-input power system stabilizer (PSS), namely PSS4B. An experience of dynamic instability [4] has analyzed in this paper. The method of analysis was to determine stability by the calculation of the Eigen values of the system. De Mello [5] has explored the phenomenon of stability of synchronous machines under small perturbations by examining the case of single machine connected to an infinite bus through external reactance. The design of PSS for single machine connected to an infinite bus has been described [6] using fast out- put sampling feedback. A step-up transformer is used to set up a modified Heffron-Philips (ModHP) model. The PSS design based on this model utilizes signals available within the generating station [7]. An augmented PSS [8] is described which extends the performance capabilities into the weak tie-line case. E.V. Larsen and D.A. Swann [9] have presented in their 3 paper titled 'Applying power system stabilizer - I, II, III' the history of power system stabilizer and its role in a power system. Practical means have been developed using Eigen value [10] analysis techniques to guide the selection process. An extended quasi-steady-state model [11] has presented that includes low-frequency inter-area oscillations which can be used effectively for the design of power system stabilizers. Yoshinari Sudou, Akira Takeuchi, and others [12] have describe a PSS that can dmp inter-area modes of a wide band more effectively than the currently available PSS. P. Kundur, M.Klein, G.J.Rogers and M.S. Zywno [13] have presented the details of power system stabilizer control design for a generating station in Ontario with the objective to enhance overall system stability. M.Klein, G.J.Rogers, S. Moorty and P. Kundur[14] in their paper shown that the PSS location and the voltage characterstics of the system loads are significant factors to increase the damping of inter-area oscillations. Ziad M.M. Ali and Alexander I. Malikov [15] have suggested robust techniques to design power system stabilizer. Joe H. Chow,George E. Boukarim and Alexander Murdoch [16] have presented three PSS design projects, based on the root-locus, frequency-response and state space methods. P. Kundur [17] has provided an account of the measures and procedures that contribute to the effective application of power system stabilizer in order to enhance system reliability.

Lin [18] proposed a fuzzy logic power system stabilizer which could shorten the tuning process of fuzzy rules and membership functions. The proposed PSS has two stages, first stage develops a proportional derivative type PSS, in the second stage it is transformed into Fuzzy Logic PSS. Roosta, A.R, [19] have described three proposed types of fuzzy control algorithms and tested in the case of single machine connected to the network for various types of disturbance. M.L. Kothari, T. Kumar [20] have presented a new approach for designing a fuzzy logic power system stabilizer such that it improves both transient and dynamic stabilities. Here they have considered FLPSS based on 3, 5 and 7 MFs of Gaussian shape. T. Hussein [21] has described an indirect variable- structure adaptive fuzzy controller as a power system stabilizer to damp inter-area modes of oscillation following disturbances in power systems. S.K. Yee and J.V. Milanovic [22] have proposed a decentralized fuzzy logic controller using a systematic analytical method based on a performance index N. Gupta and S.K. Jain [23] have described the performance of single machine infinite bus system with fuzzy power system stabilizer. Here the generator is represented by the standard K-coefficients as second order systems and the performance is investigated for Trapezoidal, Triangular Gaussian membership functions of input and output variables. M. Ramirez, O.P. Malik [24] have described a simplified fuzzy logic controller (SFLC) with a significantly reduced set of fuzzy rules, small number of tuning parameters and simple control algorithm and structure. T. Hussein [25] has presented a robust adaptive fuzzy controller as a power system stabilizer to damp inter-area modes of oscillation following disturbances in power systems. H.M. Behbehani [26] have used fuzzy logic principles to develop supervisory power system stabilizers to enhance damping of inter-area oscillations to improve stability and reliability of power system subjected to disturbances. N.Nallathambi and P. N. Neelakantan [27] present a study of fuzzy logic power system stabilizer for stability enhancement of a two-area four machine system. A. Singh [28] has described the design of a fuzzy logic based controller to counter the small-signal oscillatory instability in power systems. Taliyat et al. [29] proposed an augmented fuzzy PSS. Abdelazim and Malik [30] proposed a self learning fuzzy logic power system stabilizer. N. I. Voropai and P. V. Etingov [31] have presented an application of FLPSS to the large electric power system. P. Hoang and K. Tomosovic [32] have presented a systematic approach to fuzzy logic control design. Hamid A. Toliyat and others [33.] have introduced an augmented Fuzzy Power System Stabilizer which is helpful to enhance power system dynamics. M. A. M. Hassan and O. P. Mallik [34] described a fuzzy logic based self tuned controller

wherein the stabilizing signal generated by the controller is computed using a standard fuzzy membership function and a self tuned parameter. R. Ramya and K. Selvi [35] have presented a controller based on fuzzy logic to simulate an automatic voltage regulator to achieve the settling time quicker than conventional PSS. Similarly K. C. Rout and P. C. Panda [36] have presented fuzzy controller which enhance damping of the system much faster. D. K. Sambariya and Rajendra Prasad [37] have compared the performance of fuzzy logic PSS with different membership functions and concluded that Gaussian MF gave the best performance. D. Murali and M. Rajaram [38] demonstrated the response of fuzzy PSS on a multi machine power system under different operating conditions. P. Kundur and others [39] ,members of IEEE/CIGRE Joint Task Force on Stability Terms and Definitions addressed the issue of stability definition and classification in power system. P. Kundur [40] covers very wide spectrum of power system stability and control.

1.3 Outline of the Thesis

This project was carried out with the following objectives:

1) To study the nature of power system stability, excitation system, automatic voltage regulator for synchronous generator and power system stabilizer.

2) To develop a fuzzy logic based power system stabilizer which will make the system quickly stable when fault occurred in the transmission line.

3) To compare performance of fuzzy logic based power system stabilizer with conventional power system stabilizer by using simulation.

The chapter wise contributions of the thesis are given as hereunder:

Chapter 1 introduces the problem of small-signal stability in power systems, with emphasis on the low frequency oscillation phenomena occurring due to small disturbances and its mitigation by means of CPSS and Fuzzy PSS. It also presents a review of literature which discusses the relevant work in this area of tuning of PSS and lays down the motivations and objectives of the work.

Chapter 2 presents classical power system stabilizer in brief. It also presents the small-signal stability models of a single machine connected to an infinite bus (SMIB).It also described mathematical formation of the state space matrix of SMIB system.

Chapter 3 presents a frequency response method for the design of a conventional power system stabilizer (CPSS) in the frequency domain. It also describes components of CPSS and function of each component to tune the PSS.

Chapter 4 presents briefly the fuzzy logic control theory and need for implementing fuzzy controller in the design of PSS. It also describes how to design a fuzzy logic controller to be used in Fuzzy based PSS to mitigate power system oscillation.

Chapter 5 presents case study and discussions for without excitation system, with excitation system only, with conventional PSS, with fuzzy logic based PSS and a comparison has been made between conventional PSS and fuzzy logic based PSS with regard to damping power system oscillations.

Chapter 6 presents conclusion and suggestions for future works.

CHAPTER -2

MODELLING OF SMIB SYSTEM

For stability assessment of power system adequate mathematical models describing the system are needed. The models must be computationally efficient and be able to represent the essential dynamics of the power system. The mathematical model for small signal analysis of synchronous machine, excitation system and the lead-lag power system stabilizer are briefly reviewed. A general system configuration for the study of small signal performance of a single machine connected to a large system through transmission lines is shown in Figure 2.1 (a)

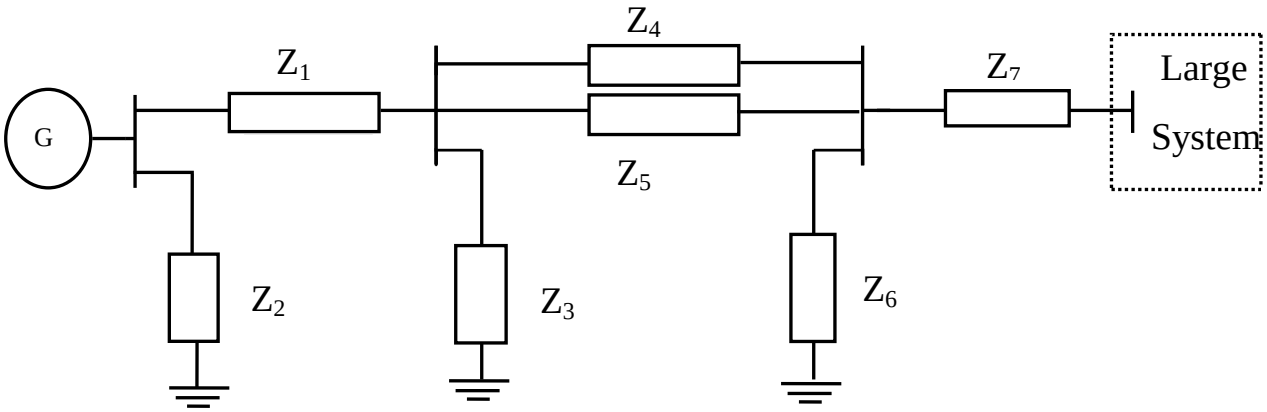

(a) General Configuration

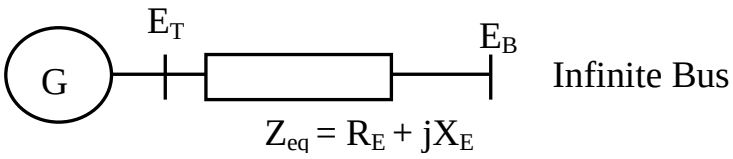

(b) Equivalent System

Figure 2.1: General configuration of SMIB System.

For the purpose of analysis, the system of Figure 2.1 (a) may be reduced to the form of Figure 2.1 (b) by using Thevenin's equivalent of the transmission network external to the machine and the adjacent transmission. Because of the relative size of the system to which the machine is

supplying power, dynamics associated with the machine will cause virtually no change in the voltage and frequency of Thevenin's voltage E_B. Such a voltage source of constant frequency is referred to as an infinite bus.

2.1 Equations of Motions

The equations of central importance in power system stability analysis are the rotational inertia equations describing the effect of unbalance between the electromagnetic torque and the mechanical torque of the individual machines.

When there is an unbalance between the torques acting on the rotor, the net torque causing acceleration (or deceleration) is

$$T_a = T_m - T_e$$

where T_a = accelerating torque in N-m

T_m = mechanical torque in N-m

T_e = electromagnetic torque in N-m

The combined inertia of the generator and prime mover is accelerated by the unbalance in the applied torques. Hence, the equation of motion is

$$\mathrm{J}\frac{d\omega_m}{dt} = T_a = T_m - T_e$$

Where J = combined moment of inertia of generator and turbine, kg-m^2

ω_m = angular velocity of the rotor, mech. rad/s

t = time in sec

The above equation can be normalized in terms of per unit inertia constant *H*, defined as the kinetic energy in watt-seconds at rated speed divided by the VA base. Using ω_{0m} to denote rated angular velocity in mechanical radians per seconds, the inertia constant is

$$H = \frac{1}{2}\frac{j\omega_{0m}^2}{VA_{base}}$$

The moment of inertia J in terms of H is

$$\mathrm{J} = \frac{2H}{\omega_{0m}^2} VA_{base}$$

$$\frac{2H}{\omega_{0m}^2} VA_{base} \frac{d\omega_m}{dt} = T_m - T_e$$

so

$$2H \frac{d}{dt}\left(\frac{\omega_m}{\omega_{0m}}\right) = \frac{T_m - T_e}{VA_{base}/\omega_{0m}}$$

Noting that $T_{base} = VA_{base}/\omega_{0m}$, the equation of motion in per unit form is

$$2H \frac{d\bar{\omega}_r}{dt} = \bar{T}_m - \bar{T}_e$$

$$\bar{\omega}_r = \frac{\omega_m}{\omega_m} = \frac{\omega_r}{\omega_0}$$

Where ω_r angular velocity of the rotor is in electrical rad/s, ω_0 is its rated value, and p_f is number of field poles.

If δ is the angular position of the rotor in electrical radians with respect to synchronously rotating reference and δ_0 is its value at t = 0.

$$\delta = \omega_r t - \omega_0 t + \delta_0$$

Taking the time derivative, we have

$$\frac{d\delta}{dt} = \omega_r - \omega_0$$

$$= \Delta\omega_r$$

and

$$\frac{d^2\delta}{dt^2} = \frac{d\omega_r}{dt} = \frac{d(\Delta\omega_r)}{dt}$$

$$= \omega_0 \frac{d\bar{\omega}_r}{dt} = \omega_0 \frac{d(\Delta\bar{\omega}_r)}{dt}$$

substituting for $d\bar{\omega}_r/dt$ given by the above equation

$$\frac{2H}{\omega_0} \frac{d^2\delta}{dt^2} = \bar{T}_m - \bar{T}_e$$

By taking damping torque into consideration swing equation becomes

$$\frac{2H}{\omega_0} \frac{d^2\delta}{dt^2} = \bar{T}_m - \bar{T}_e - K_D \Delta\bar{\omega}_r \qquad (2.1)$$

and

$$\Delta\bar{\omega}_r = \frac{\Delta\omega_r}{\omega_0} = \frac{1}{\omega_0} \frac{d\delta}{dt}$$

Equation 2.1 represents the equation of motion of a synchronous machine.

2.2 Classical Model of Generator

With the generator represented by the classical model all resistances neglected, the system representation is as shown in Figure 2.2.

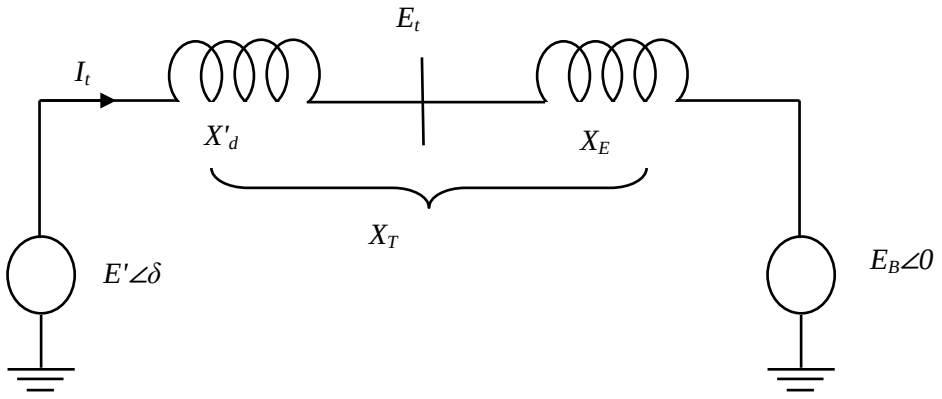

Figure 2.2: Classical Model of synchronous generator

Here E' is the voltage behind X'_d. Its magnitude is assumed to remain constant at the pre-disturbance value. Let δ be the angle by which E' leads the infinite but voltage E_B. As the rotor oscillates during a disturbance, δ changes

with E' as reference phasor,

$$\tilde{I}_t = \frac{E' \angle 0^0 - E_B \angle -\delta}{jX_T} = \frac{E' - E\ (\cos\delta - j\sin\delta)}{jX_T}$$

The complex power behind X'_d is given by

$$S' = P + jQ' = \tilde{E}'\tilde{I}_t^*$$

$$= \frac{E'E_{B\sin\delta}}{X_T} + j\left(\frac{E' - E_{B\cos\delta}}{X_T}\right)$$

With stator resistance neglected, the gap power (P_e) is equal to the terminal power (P). In per unit, the air-gap torque to the air-gap power, hence,

$$T_e = P = \frac{E'E_B}{X_T}\sin\delta$$

Linearizing about an initial operating condition represented by $\delta = \delta_0$ yields

$$\Delta T_e = \frac{\partial T_e}{\partial \delta}\Delta\delta = \frac{E'E_B}{X_T}\cos\delta_0(\Delta\delta)$$

The equation of motion in per unit is

$$p\Delta\omega_r = \frac{1}{2H}(T_m - T_e - K_D\Delta\omega_r) \qquad (2.2)$$

$$p\delta = \omega_0\Delta\omega_r \qquad (2.3)$$

Where $\Delta\omega_r$ is the per unit speed deviation, δ is rotor angle in electrical radians, ω_0 is the base rotor electrical speed in radians per second, and p is the differential operator with respect to time.

Linearizing equations 2.2 and 2.3 and substituting for ΔT_e

$$p\Delta\omega_r = \frac{1}{2H}\left[\Delta T_m - K_s\Delta\delta - K_D\Delta\omega_r\right]$$

Where K_s is the synchronizing torque coefficient given by

$$K_s = \left(\frac{E'E_B}{X_T}\right)\cos\delta_0$$

$$p\Delta\delta_r = \omega_0\Delta\omega_r$$

$$\frac{d}{dt}\begin{bmatrix}\Delta\omega_r \\ \Delta\delta\end{bmatrix} = \begin{bmatrix}\frac{-K_D}{2H} & \frac{-K_s}{2H} \\ \omega_0 & 0\end{bmatrix}\begin{bmatrix}\Delta\omega_r \\ \Delta\delta\end{bmatrix} + \begin{bmatrix}\frac{1}{2H} \\ 0\end{bmatrix}\Delta T_m \qquad (2.4)$$

This is the form $\dot{x}$= **Ax + bu**. The elements of the state matrix A are seen to be dependent on the system parameters K_D, H, X_T, and the initial operating conditions represented by the values of E'.

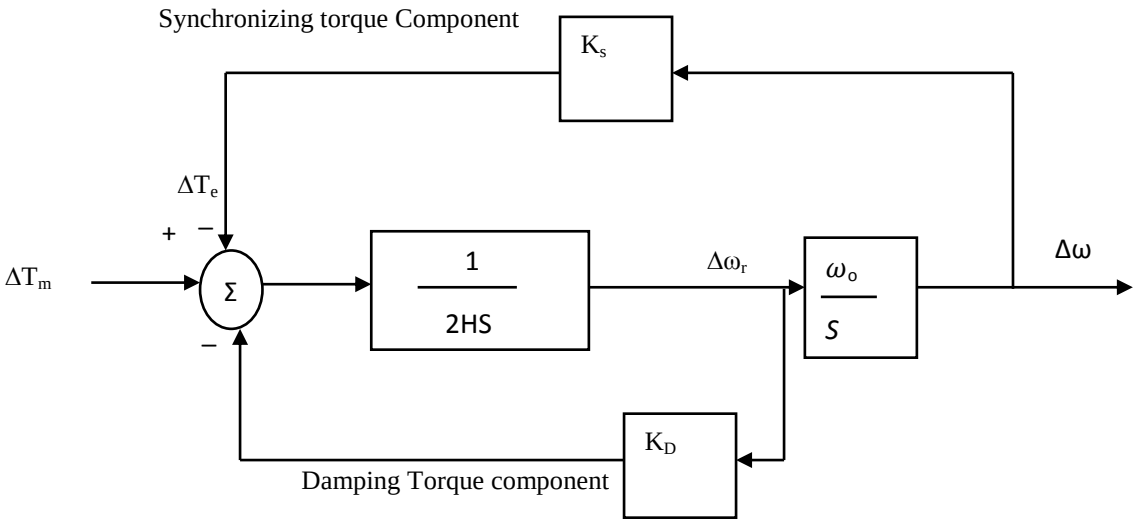

Figure 2.3 **:** Block diagram of a SMIB system with classical generator model

and the block diagram representation shown in Figure 2.3

From the block diagram

$$\Delta\delta = \frac{\omega_0}{s}\left[\frac{1}{2Hs}(-K_s\Delta\delta - K_D\Delta\omega_r + \Delta T_m)\right]$$

$$= \frac{\omega_0}{s}\left[\frac{2}{2Hs}\left(-K_s\Delta\delta - K_D s\frac{\Delta\delta}{\omega_0} + \Delta T_m\right)\right]$$

Therefore, the characteristic equation is given by

$$s^2 + \frac{K_D}{2H}s + \frac{K_s\omega_0}{2H} = 0$$

This is of the general form

$$s^2 + 2\xi\omega_n s + \omega_n^2 = 0$$

Hence, the un-damped natural frequency is

$$\omega_n = \sqrt{K_s\frac{\omega_0}{2H}} \quad \text{rad/s}$$

and the damping ratio is

$$\xi = \frac{1}{2}\frac{K_D}{2H\omega_n}$$
$$= \frac{1}{2}\frac{K_D}{\sqrt{K_s 2H\omega_0}}$$

As the synchronizing torque coefficient K_s increases, the natural frequency increases and the damping ration decreases. An increase in damping torque coefficient $K_{D,}$ increases the damping ratio,whereas an increase in inertia constant decreases both ω_n and ξ.

2.3 Synchronous machines field circuit dynamics

Let us analyze the system performance including the effect of field flux variation. The amortisseurs effect is neglected and the field voltage is assumed constant.

Synchronous machine equations

As in the case of the classical generator model, the acceleration equations are given by

$$p\Delta\omega_r = \frac{1}{2H}\left(T_m - T_e - K_{D\Delta}\omega_r\right) \quad (2.5)$$

$$p\delta = \omega_0\Delta\omega_r \quad (2.6)$$

where $\omega_0 = 2\pi f_0$ elec.rad/s.

As the field circuit dynamic equation is

$$p\psi_{fd} = \omega_0\left(e_{fd} - \omega_0 R_{fd} i_{fd}\right)$$

$$= \frac{\omega_0 R_{fd}}{L_{adu}} E_{fd} - \omega_0 R_{fd} i_{fd} \quad (2.7)$$

Where E_{fd} is the exciter output voltage. Equation 2.4 to 2.7 describe the dynamics of the synchronous machine with $\Delta\omega_r$, δ, ψ_{fd} as the state variables.

With amortisseurs neglected, the equivalent circuits relating the machine flux linkages and current are as shown in figure 2.4.

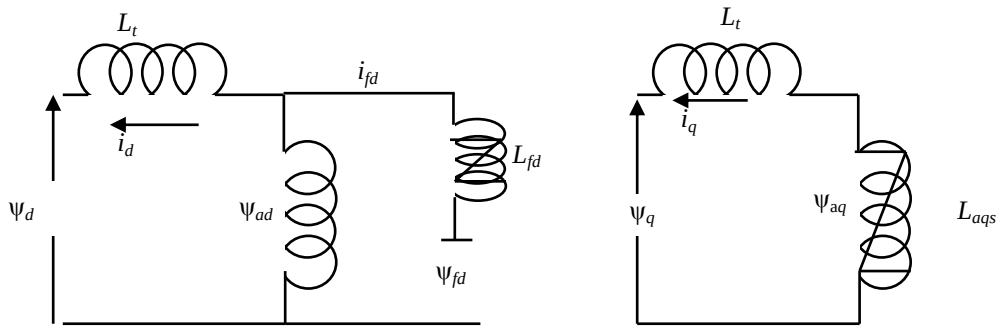

Figure 2.4: Equivalent circuit showing the flux linkage and current

The stator and rotor flux linkages are given by

$$\psi_d = -L_i i_d + L_{ads}\left(-i_d + i_{fd}\right)$$

$$= -L_i i_d + \psi_{ad} \quad (2.8)$$

$$\psi_q = -L_i i_q + L_{aqs}\left(-i_q\right)$$

$$= -L_i i_q + \psi_{aq} \quad (2.9)$$

$$\psi_{fd} = -L_{ads}(-i_d + i_{jd}) + L_{fd} i_{fd}$$

$$= \psi_{ad} + L_{fd} i_{fd} \quad (2.10)$$

In the above equations ψ_{ad} and ψ_{aq} are the air-gap (mutual) flux linkages, and L_{ads} and L_{aqs} are the saturated values of the mutual inductances.

Hence

$$i_{fd} = \frac{\psi_{fd} - \psi_{ad}}{L_{fd}}$$

The d-axis mutual flux linkage can be written in terms of ψ_{fd} and i_d as follows:

$$\psi_{ad} = -L_{ads} i_d + L_{ads} i_{fd}$$

$$= -L_{ads} i_d + \frac{L_{ads}}{L_{fd}}(\psi_{fd} - \psi_{ad})$$

$$= L'_{ads}\left(-i_d + \frac{\psi_{fd}}{L_{fd}}\right) \quad (2.11)$$

Since there are no rotor circuits considered in the q- axis, the mutual flux linkage is given by

$$\psi_{aq} = -L_{aqs} i_q \quad (2.12)$$

The air-gap torque is

$$T_e = \psi_d i_q - \psi_q i_d$$

$$= \psi_{ad} i_q - \psi_{aq} i_d \quad (2.13)$$

With $p\psi$ terms and speed variations neglected, the stator voltage equations are

$$e_d = -R_a i_d - \psi_q$$

$$= -R_a i_d + (L_i i_q - \psi_{aq}) \quad (2.14)$$

$$e_q = -R_a i_d + \psi_d$$
$$= -R_a i_q - (L_i i_d - \psi_{ad}) \quad (2.15)$$

The machine terminal and infinite bus voltage in terms of the d-axis and q-axis components are

$$\tilde{E}_t = e_d + j e_q$$
$$\tilde{E}_B = E_{Bd} + j E_{Bq}$$

Also

$$\tilde{E}_t = \tilde{E}_B + (R_E + jX_E)\,\tilde{I}_t$$
$$(e_d + j e_q) = (E_{Bd} + j E_{Bq}) + (R_E + jX_E)(I_d + j i_q)$$

Resolving into d-axis and q-axis components gives

$$e_d = R_E i_d + X_E i_q + E_{Bd}$$
$$e_q = R_E i_q - X_E i_d + E_{Bq}$$

where

$$E_{Bd} = E_B \sin\delta$$
$$E_{Bq} = E_B \cos\delta$$

After re-arranging the equations

$$i_d = \frac{X_{Tq}\left[\psi_{fd}\left(\frac{L_{ads}}{L_{ads} + L_{fd}}\right) - E_B cos\delta\right] - R_T E_B sin\delta}{D} \quad (2.16)$$

$$i_d = \frac{R_T\left[\psi_{fd}\left(\frac{L_{ads}}{L_{ads} + L_{ads}}\right) - E_B cos\delta\right] + X_{Td} E_B sin\delta}{D} \quad (2.17)$$

$$R_T = R_a + R_E$$

$$X_{Tq} = X_E + \left(L_{aqs} + L_l\right) = X_E + X_{qs}$$

$$X_{Td} = X_E + \left(L'_{ads} + L_l\right) = X_E + X'_{ds}$$

$$D = R_T^2 + X_{Tq} + X_{Td} \tag{2.18}$$

The reactances X_{qs} and X'_{ds} are saturated values. In per unit they are equal to the corresponding inductances.

Expressing Equations 2.16 and 2.17 in terms of perturbed values,

$$\Delta i_d = m_1 \Delta\delta + m_2 \Delta\psi_{fd} \tag{2.19}$$

$$\Delta i_q = n_1 \Delta\delta + n_2 \Delta\psi_{fd} \tag{2.20}$$

$$m_1 = \frac{E_B\left(X_{Tq} Sin\delta_0 - R_T cos\delta_0\right)}{D}$$

$$n_1 = \frac{E_B(R_T sin\delta_0 + X_{Td} cos\delta_0)}{D}$$

$$m_2 = \frac{X_{Tq}}{D} \frac{L_{ads}}{\left(L_{ads} + L_{fd}\right)}$$

$$n_2 = \frac{R_T}{D} \frac{L_{ads}}{\left(L_{ads} + L_{fd}\right)} \tag{2.21}$$

By linearizing Equations 2.11 and 2.12 and substituting in them the above expressions for Δi_d and Δi_q we get

$$\Delta\psi_{ad} = L'_{ad}\left(-\Delta i_d + \frac{\Delta\psi_{fd}}{L_{fd}}\right)$$

$$= \left(\frac{1}{L_{fd}} - m_2\right) L'_{ads}\Delta\psi_{fd} - m_1 L'_{ads}\Delta\psi \qquad (2.22)$$

$$\Delta\psi_{aq} = -L_{ads}\Delta i_q$$

$$= -n_2 L_{aqs}\Delta\psi_{fd} - n_1 L_{aqs}\Delta\delta \qquad (2.23)$$

Linearizing equation 2.10 and substituting for ψ_{ad} from equation 2.22 gives

$$\Delta i_{fd} = \frac{\Delta\psi_{fd} - \Delta\psi_{ad}}{L_{fd}}$$

$$= \frac{1}{L_{fd}}\left(1 - \frac{L'_{ads}}{L_{fd}} + m_2 L'_{ads}\right)\Delta\psi_{fd} + \frac{1}{L_{ads}} m_1 L'_{ads}\Delta\delta \qquad (2.24)$$

so $\Delta T_e = \psi_{ad0}\Delta i_q + i_{q0}\Delta\psi_{ad} - \psi_{aq0}\Delta i_d - i_{d0}\Delta\psi_{aq}$

Substituting for $\Delta i_d, \Delta i_q, \Delta\psi_{ad}$ and $\Delta\psi_{aq}$ from equation 2.19 to 2.23 we obtain

$$\Delta T_e = K_1\Delta\delta + K_2\Delta\psi_{fd} \qquad (2.25)$$

Where

$$K_1 = n_1\left(\psi_{ad0} + L_{aqs} i_{do}\right) - m_1\left(\psi_{aq0} + L'_{ads} i_{q0}\right) \qquad (2.26)$$

$$K_2 = n_2\left(\psi_{ad0} + L_{aqs} i_{d0}\right) - m_2\left(\psi_{aq0} + L'_{ads} i_{q0}\right) + \frac{L'_{ads}}{L_{fd}} i_{q0} \qquad (2.27)$$

$$\begin{bmatrix} \Delta\dot{\omega}_r \\ \Delta\dot{\delta} \\ \Delta\dot{\psi}_{fd} \end{bmatrix} = \begin{bmatrix} a_{11} & a_{12} & a_{13} \\ a_{21} & 0 & 0 \\ 0 & a_{32} & a_{33} \end{bmatrix} \begin{bmatrix} \Delta\omega_r \\ \Delta\delta \\ \Delta\psi_{fd} \end{bmatrix} + \begin{bmatrix} b_{11} & 0 \\ 0 & 0 \\ 0 & b_{32} \end{bmatrix} \begin{bmatrix} \Delta T_m \\ \Delta E_{fd} \end{bmatrix} \qquad (2.28)$$

where

$$a_{11} = -\frac{K_D}{2H}$$

$$a_{12} = -\frac{K_1}{2H}$$

$$a_{13} = -\frac{K_2}{2H}$$

$$a_{21} = \omega_0 = 2\pi f_0$$

$$a_{32} = -\frac{\omega_0 R_{fd}}{L_{fd}} m_1 L'_{ads}$$

$$a_{33} = -\frac{\omega_0 R_{fd}}{L_{fd}} \left[1 - \frac{L'_{ads}}{L_{fd}} + m_2 L'_{ads}\right]$$

$$b_{11} = \frac{1}{2H}$$

$$b_{32} = \frac{\omega_0 R_{fd}}{L_{ads}}$$

and ΔT_m and Δf_d depends on prime-mover and excitation control. With constant mechanical input torque, ΔT_m = 0 and ΔE_{fd} = 0 with constant exciter output voltage.

Figure 2.5 shows the block diagram representation of the small-signal performance of the system. In this representation, the dynamic characteristics of the system are expressed in terms of the so-called 'K' constants. The basis for the block diagram and the expressions for the associated constants are developed below:

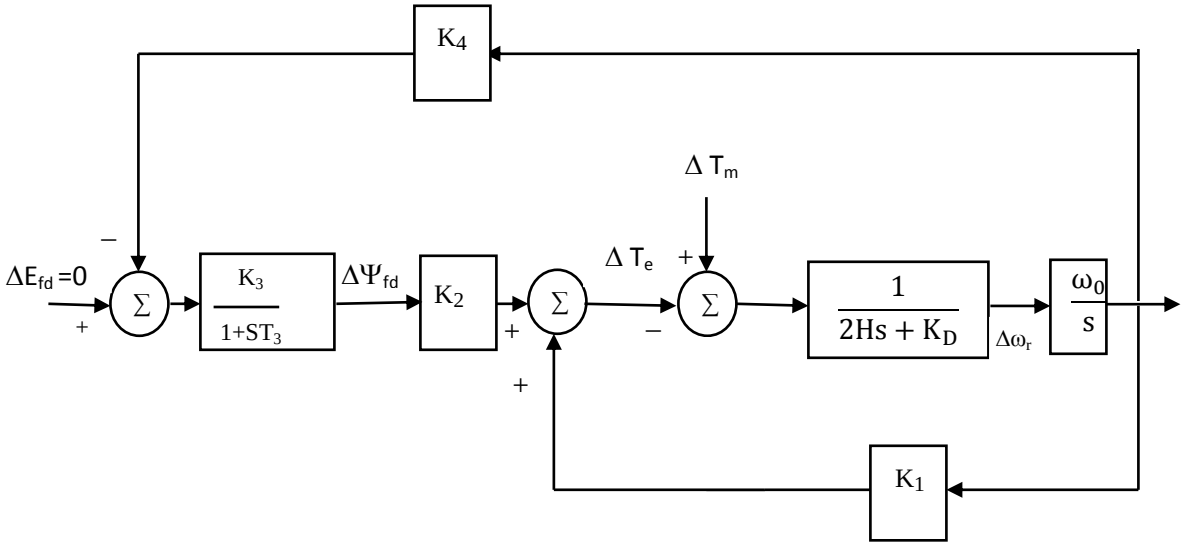

Figure 2.5 : Block Diagram Representation with Constant E_{fd}

From equation 2.25, the change in air gap torque as a function of Δδ and $\Delta\psi_{fd}$ as follows:

$$\Delta T_e = K_1 \Delta\delta + K_2 \Delta\psi_{fd}$$

Where

$$K_1 = \frac{\Delta T_e}{\Delta\delta} \text{ with constant } \psi_{fd}$$

$$K_2 = \frac{\Delta T_e}{\Delta\psi_{fd}} \text{ with constant rotor angle } \delta$$

The component of torque given by $K_1\Delta\delta$ is in phase with Δδ and hence represents a synchronizing torque component.

The component of torque resulting from variations in fields flux linkage is given by $K_2\Delta\psi_{fd}$

The variation of ψ_{fd} is determined by the field circuit dynamic equation.

$$p\Delta\psi_{fd} = a_{32}\Delta\delta + a_{33}\Delta\psi_{fd} + b_{32}\Delta E_{fd}$$

$$\Delta\psi_{fd} = \frac{K_3}{1+pT_3}\left[\Delta E_{fd} - K_4\Delta\delta\right]$$

$$K_3 = -\frac{b_{32}}{a_{33}}$$

$$K_4 = -\frac{a_{32}}{b_{33}}$$

$$T_3 = -\frac{1}{a_{33}} = K_3 T'_{do}\frac{L_{adu}}{L_{ffd}} \qquad (2.29)$$

Expression for the K Constants in the expanded form

As $K_1 = n_1\left(\psi_{ad0} + L_{aq}i_{d0}\right) - m_1\left(\psi_{aq0} + L'_{ads}i_{q0}\right)$

From Equation 2.15 the first term in parentheses in the above expression for K_1 may be written as

$$\psi_{ad0} + L_{aqs}i_{d0} = e_{qo} + R_a i_{qo} + X_{qs}i_{do} = E_{q0}$$

Where E_{q0} is the pre-disturbance value of the voltage behind $R_a + jX_q$. The second term in parentheses in the expression for K_1 may be written as

$$\psi_{ad0} + L'_{aqs}i_{d0} = L'_{aqs}i_{d0} + L'_{aqs}i_{d0}$$
$$= -\left(X_q - X'_d\right)i_{q0}$$

Substituting for n_1, m_1 from equation 2.21 and for the terms given by above equations in the expression for K_1, yields

$$K_1 = \frac{E_B E_{q0}}{D}(R_T sin\delta_0 + X_{Td} cos\delta_0) +$$

$$\frac{E_B i_{q0}}{D}\left(X_q - X'_d\right)\left(X_{Tq} sin\delta_0 - R_T cos\delta_0\right)$$

Similarly, the expanded form of the expression for the constant K_2 is

$$K_2 = \frac{L_{ads}}{L_{ads} + L_{ads}}\left[\frac{R_T}{D}E_{q0} + \left(\frac{X_{Tq}\left(X_q - X'_d\right)}{D} + 1\right) iq_0\right]$$

and

$$\begin{aligned} a_{33} \quad &= -\omega_0 \frac{R_{fd}}{L_{fd}}\left[1 - \frac{L_{ads}}{L_{ads} + L_{fd}} + \frac{X_{Tq}}{D}\frac{L_{ads}}{\left(L_{ads} + L_{fd}\right)}\frac{L_{ads}L_{fd}}{\left(L_{ads} + L_{fd}\right)}\right] \\ &= -\omega_0 \frac{R_{fd}}{L_{ads} + L_{fd}}\left[1 + \frac{X_{Tq}}{D}\frac{L_{ads}^2}{\left(L_{ads} + L_{fd}\right)}\right] \\ &= -\omega_0 \frac{R_{fd}}{L_{ads} + L_{fd}}\left[1 + \frac{X_{Tq}}{D}\left(X_d - X'_d\right)\right] \end{aligned}$$

After arranging the equations

$$\begin{aligned} K_3 &= \frac{L_{ads} + L_{fd}}{L_{adu}}\frac{1}{1 + \frac{X_{Tq}}{D}\left(X_d - X'_d\right)} \\ &= \frac{T'_{d0s}}{1 + \frac{X_{Tq}}{D}\left(X_d - X'_d\right)} \end{aligned}$$

Where T'_{d0s} is the saturated value of T'_{d0}. Similarly

$$a_{32} = -\omega_0 \frac{R_{fd}E_B}{L_{fd}D}\left(X_{Tq}\sin\delta_0 - R_T\cos\delta_0\right)\frac{L_{ads}L_{fd}}{L_{ads} + L_{fd}}$$

Thus

$$K_4 = L_{ads}\frac{L_{ads}}{(L_{ads}+L_{fd})}\frac{E_B}{D}\left(X_{Tq}\sin\delta_0 - R_T\cos\delta_0\right)$$

Representation of Saturation in Stability Studies

In the representation of magnetic saturation for stability studies the following assumptions are usually made:

(a) The leakage inductances are independent of saturation. The leakage fluxes are in air for a considerable portion of their paths so that they are not significantly affected by saturation of the iron portion. As a result, the only elements that saturated are the mutual inductances L_{ad} and L_{aq}.

(b) The leakage fluxes do not contribute to the iron saturation. The leakage fluxes are usually small and their paths coincide with that of the main flux for only a small part of its path. By this assumption, saturation is determined by the air-gap flux linkage.

(c) The Saturation relationship between the resultant air-gap flux and the m.m.f. under loaded conditions is the same as under no-load conditions. This allows the saturation characteristics to be represented by the open-circuit saturation curve, which is usually the only saturation data readily available.

(d) There is no magnetic coupling between the d- and q- axes as a result nonlinearities introduced by saturation; i.e., currents in the windings of one axis do not produce flux that link with the windings of the other axis.

With the above assumptions, the effect of saturation may be represented as

$$L_{ad} = K_{sd}L_{adu}$$

$$L_{aq} = K_{sq}L_{aqu}$$

Where $L_{adu}\ and\ L_{aqu}$ are the unsaturated values of L_{ad} and L_{aq}. The saturation factors K_{sd} and K_{sq} identifies the degree of saturation in the d- and q-axis, respectively.

Effect of field flux linkage variation on system stability

With constant field voltage $(\Delta E_{fd} = 0)$, the field variations are caused only by feedback of Δδ through the coefficient K_4. This represents the demagnetizing effect of the armature reaction.

The change in air- gasp torque due to filed flux variation caused by rotor angle changes is given by

$$\frac{\Delta T_e}{\Delta \delta} = -\frac{K_2 K_3 K_4}{1 + sT_3}$$

The constants $K_2, K_3 and\ K_4$ are usually positive. The contribution of $\Delta\psi_{fd}$ to synchronizing and damping torque components depends on the oscillating frequency as discussed below:

(a) In the steady state and at very low oscillating frequencies (sjω→0):

$$\Delta T_e\ due\ to\ \Delta\psi_{fd=-K_2K_3K_4\Delta\delta}$$

The field flux variation due to Δδ feedback (i.e., due to armature reaction) introduce a negative synchronizing torque components. The system becomes monotonically unstable when this exceeds $K_1\Delta\delta$. The steady state stability limit is reached when

$$K_2 K_3 K_4 = K_1$$

(b) At oscillating frequencies much higher than $1/T_3$:

$$\Delta T_e = \frac{K_2 K_3 K_4}{j\omega T_3}\Delta\delta$$

$$= \frac{K_2 K_3 K_4}{\omega T_3} j\Delta\delta$$

Thus, the component of air-gap torque due to $\Delta\psi_{fd}$ is 90^0 ahead of Δδ or in phase with Δω. Hence, $\Delta\psi_{fd}$ result in a positive damping torque component.

(c) At typical machine oscillating frequencies of about 1 Hz ($2\pi\ rad/s$). $\Delta\psi_{fd}$ results in a positive damping torque component and a negative synchronizing torque component. The net effect is to reduce slightly the synchronizing torque component and increase the damping.

Special Situations with K_4 negative

The coefficient K_4 is normally positive. As long as it is positive the effect of field flux variation due to armature reaction ($\Delta\psi_{fd}$ with constant E_{fd}) is to introduce a positive damping torque component. However there can be situations where K_4 is negative. This is the situation when hydraulic generator without damper windings is operating at light load and is connected by a line relatively high resistance to reactance ratio to a large system.

Also K_4 can be negative when a machine is connected to a large local load, supplied partly by the generator and partly by the remote large system. Under such conditions, the torques produced by indeed currents in the fields due to armature reaction have components out of phase with $\Delta\omega$, and produce negative damping.

2.4 Effect of Excitation System

The main control function of the excitation system is to regulate the generator terminal voltage. This is accomplished by adjusting the field voltage in response to terminal voltage variations. A typical excitation system includes a voltage regulator, an exciter, protective circuits, limiters, and measurement transducers. The voltage regulator processes the voltage deviations from a desired set point and adjusts the required input signals to exciter, which provides the dc voltage and current to the field windings, to take corrective action.

The input control signal to the excitation system is normally the generator terminal voltage E_t. The E_t is not a state variable .Therefore, E_t has to be expressed in terms of the state variables $\Delta\omega_r$, $\Delta\delta$ and ψ_{fd}.

As
$$\Delta E_t = \frac{e_{d0}}{E_{t0}}\Delta e_d + \frac{e_{q0}}{E_{t0}}\Delta e_q \qquad (2.30)$$

In terms of the perturbed values, Equations 2.14 and 2.15 may be written as

$$\Delta e_d = -R_a\Delta i_d + L_l\Delta i_q - \Delta\psi_{aq}$$

$$\Delta e_q = -R_a\Delta i_q - L_l\Delta i_d + \Delta\psi_{ad}$$

So,

$$K_5 = \frac{e_{d0}}{E_{t0}}\left[-R_a m_1 + L_l n_1 + L_{aqs} n_1\right] + \frac{e_{q0}}{E_{t0}}\left[-R_a n_2 - L_l m_1 - L'_{ads} m_1\right] \quad (2.31)$$

$$K_6 = \frac{e_{d0}}{E_{t0}}\left[-R_a m_2 + L_l n_2 + L_{aqs} n_2\right] + \frac{e_{q0}}{E_{t0}}\left[-R_a n_2 - L_l m_2 - L'_{ads}\left(\frac{1}{L_{fd}} - m_2\right)\right] \quad \ldots\ldots (2.32)$$

For the purpose of illustration and examination of the influence on small signal stability, we will consider the excitation system model shown in Figure 2.6. It is the representative of thyristor excitation system. The model shown in Figure 2.6 has been simplified to include only those elements that are considered necessary for representing a specific system. A high exciter gain is used. Parameter T_R represents the terminal voltage transducer time constant.

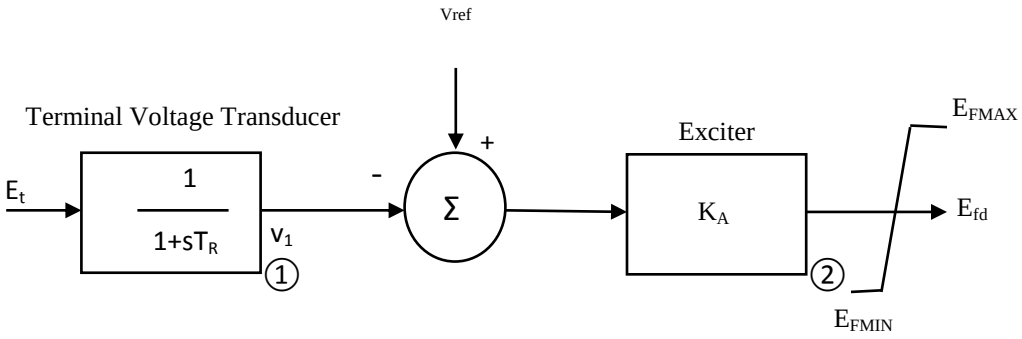

Figure 2.6: Thyristor exciter system with AVR

From block ①of Figure 3.2, using perturbed values, we have

$$\Delta v_1 = \frac{1}{1 + pT_R}\Delta E_t$$

Hence,

$$p\Delta v_1 = \frac{1}{T_R}(\Delta E_t - \Delta v_1)$$

Substituting for ΔE_t from equation 3.1, we get

$$p\Delta v_1 = \frac{K_5}{T_R}\Delta\delta + \frac{K_5}{T_R}\Delta - \frac{1}{T_R}\Delta v_1$$

From Block ②

$$E_{fd} = K_A\left(V_{ref} - v_1\right)$$

In terms of perturbed values , we have

$$\Delta E_{fd} = K_A(-\Delta v_1) \qquad (2.33)$$

The field circuit dynamic equation developed in the previous section, with the effect of excitation system included, becomes

$$p\Delta\psi_{fd} = a_{31}\Delta\omega_r + a_{32}\Delta\delta + a_{33}\Delta\psi_{fd} + a_{34}\Delta v_1 \qquad (2.34)$$

where

$$a_{34} = -b_{32}K_A = -\frac{\omega_0 R_{fd}}{L_{adu}}K_A \qquad (2.35)$$

From equation (2.34)

$$p\Delta v_1 = a_{41}\Delta\omega_r + a_{42}\Delta\delta + a_{42}\Delta\psi_{fd} + a_{44}\Delta v_1 \qquad (2.36)$$

where

$$a_{41} = 0 \;\; ; \;\; a_{42} = \frac{K_5}{T_R}$$

$$a_{43} = \frac{K_6}{T_R} \;\; ; \;\; a_{44} = -\frac{1}{T_R}$$

Since $p\Delta\omega_r$ *and* $p\Delta\delta$ are not directly affected by the exciter.

$$a_{14} = a_{24} = 0$$

The complete state model for the power system, the following form:

$$\begin{bmatrix} \Delta\dot{\omega}_r \\ \Delta\dot{\delta} \\ \Delta\dot{\psi}_{fd} \\ \Delta\dot{v}_1 \end{bmatrix} = \begin{bmatrix} a_{11} & a_{12} & a_{13} & 0 \\ a_{21} & 0 & 0 & 0 \\ 0 & a_{32} & a_{33} & a_{34} \\ 0 & a_{42} & a_{43} & a_{44} \end{bmatrix} \begin{bmatrix} \Delta\omega_r \\ \Delta\delta \\ \Delta\psi_{fd} \\ \Delta v_1 \end{bmatrix} + \begin{bmatrix} b_1 \\ 0 \\ 0 \\ 0 \end{bmatrix} \Delta T_m \qquad (2.37)$$

Block diagram including the excitation system is shown in Figure 2.7.

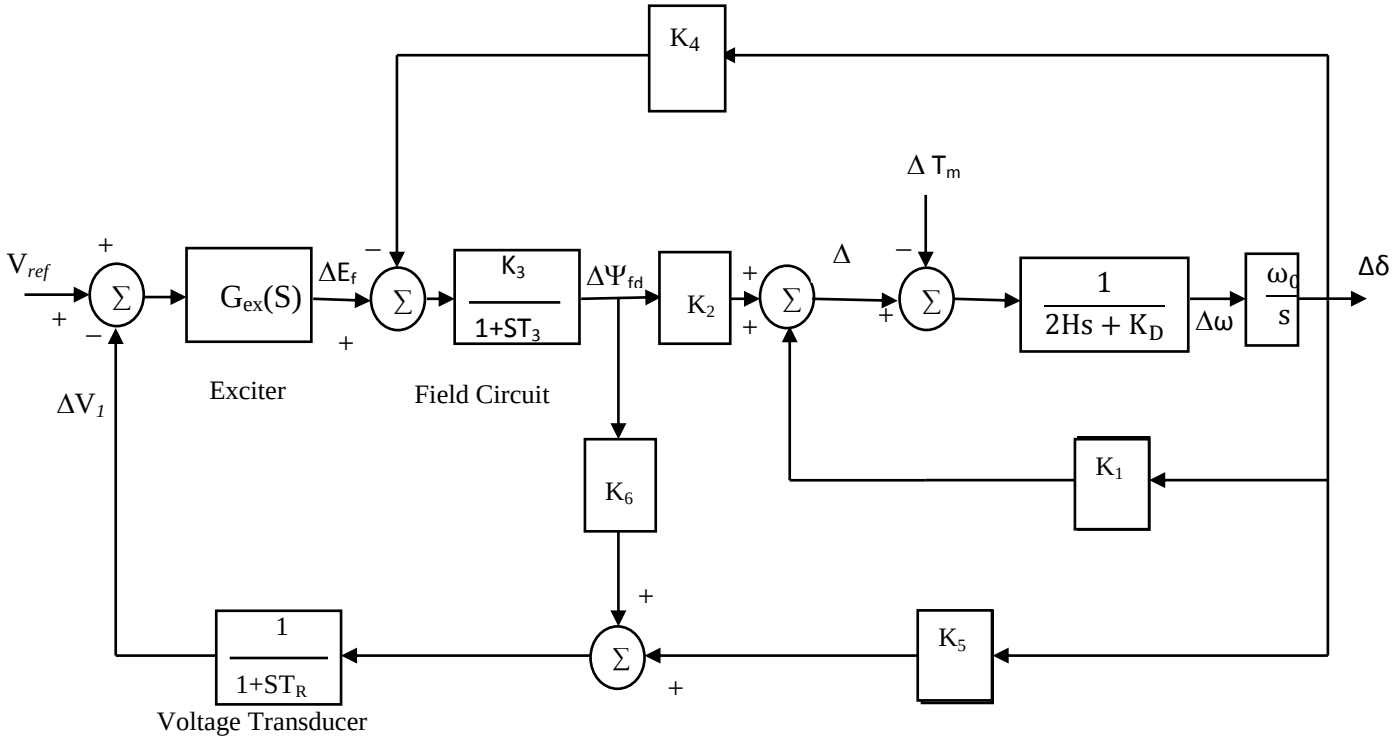

Figure 2.7 : Composite Block Diagram Representation of SMIB with AVR only

For a thyristor exciter

$$G_{ex}(s) = K_A$$

The terminal voltage error signal, which forms the input to the voltage transducer block, is given by Equation 3.1

$$\Delta E_t = K_5 \Delta\delta + K_6 \Delta\psi_{fd}$$

The coefficient K_6 is always positive , whereas K_5 can be either positive or negative , depending on the operating condition and the external network impedance R_E+jX_E. The value of K_5 has a significient bearing on the influence of the AVR on the damping of system oscillations as illustrated below.

2.5 Effect of AVR on synchronizing and damping torque components

With automatic voltage regulator action, the field flux variations are caused by the field voltage variations, in addition to the armature reaction. From the block diagram of the Figure 2.7

$$\Delta\psi_{fd} = \frac{K_3}{1+sT_3}\left[-K_4\Delta\delta - \frac{G_{ex}(s)}{1+sT_R}\left(K_5\Delta\delta + K_6\Delta\psi_{fd}\right)\right] \qquad (2.38)$$

By grouping terms involving ψ_{fd} and rearranging

$$\Delta\psi_{fd} = \frac{-K_3[K_4(1+sT_R) + K_5G_{ex}(s)]}{s^2T_3T_R + s(T_3+T_R) + 1 + K_3K_6G_{ex}(s)} \qquad (2.39)$$

The change in air-gap torque due to change in field flux linkage is

$$\Delta T_e|_{\Delta\psi fd} = K_2\Delta\psi_{fd} \qquad (2.40)$$

Constants K_2, K_3, K_4 and K_6 are usually positive, however, K_5 may take either positive or negative values. The effect of AVR on damping and synchronizing torque component is thus for primary influence by K_5 and $G_{ex}(s)$.

Example

This is illustrated by considering a specific case with parameters as follows (obtained for a given 'P' , 'Q' and | Et|

$$K_1 = 1.591 \qquad K_2 = 1.5 \qquad K_3 = 0.333$$

$$K_4 = 1.8 \qquad T_3 = 1.91$$

$$K_5 = -0.12 \qquad K_6 = 0.3 \qquad T_R = 0.02$$

$$G_{ex}(s) = K_A \qquad H = 3.0 \qquad K_D = 0.0$$

This represents a system with a thyristor exciter and system conditions such that K_5 is negative

(a) Steady state synchronizing torque coefficient:

With s= $j\omega = 0, \Delta Te \; due \; to \; \Delta\psi_{fd} \; is$

$$\Delta T_e|\Delta\psi_{fd} = \frac{-K_2K_3(K_4 + K_5K_A)}{1 + K_3K_6K_A}$$

$$\frac{0.06K_A - 0.9}{1 + 0.1K_A}\,\Delta\delta$$

Hence the synchronizing torque coefficient due to $\Delta\psi_{fd}$ is

$$\frac{0.06K_A - 0.9}{1 + 0.1\,K_A}$$

We see that the effect of the AVR is to increase the synchronizing torque component at steady state with K_A =0 (i.e. constant E_{fd})=-0.9. When K_A=15, the AVR compensates exactly for the demagnetizing effect of the armature reaction with K_A= 200, Ks($\Delta\psi_{fd}$)= 0.529 and the synchronizing torque coefficient is

$$K_s = K_1 + K_{s(\Delta\psi fd)} = 1.591 + 0.529$$

=2.12 pu torque/rad

Here, a case with K_5 negative has been considered. With a positive K_5 the AVR would have an effect opposite to the above; that is, the effect of the AVR would be to reduce the steady state synchronizing torque component.

Although a thyristor exciter has been considered in this example, the above observations apply to any type of exciter with a steady state exciter/ AVR gain equal to K_A.

(b) **Damping and synchronizing torque components at the rotor oscillation frequency**

Substituting of the numerical values applicable to the specific case under consideration

$$\Delta\psi_{fd} = \frac{-0.6 - 0.333K_5K_A - 0.012s}{0.0382s^2 + 1.93s + 1 + 0.1K_A}\Delta\delta$$

$\Delta T_e|\Delta\psi_{fd} = K_2\Delta\psi_{fd}$

$$= \frac{1.5(-0.6 - 0.333K_5K_A - 0.012s)}{0.0382s^2 + 1.93s + 1 + 0.1K_A}$$

We will assume that the rotor oscillation frequency is 10 rad/s 91,6 Hz). With s= $j\omega = j10$.

$$\Delta T_{e|\Delta\psi fd} = \frac{-0.9 - 0.5K_5K_A - j0.18}{-2.82 + 0.1K_A + j19.3}\ \Delta\delta$$

With K_5= - 0.12 and K_A= 200

$$\Delta T_{e|\Delta\psi fd} = \frac{11.1 - j0.18}{17.18 + j19.3}\Delta\delta$$

$$= 0.2804\Delta\delta - 0.3255(j\Delta\delta)$$

Thus the effect of the AVR is to increase the synchronizing torque component and decrease the damping torque component, when K_5 is negative.

The net synchronizing torque coefficient is

$K_S = K_1 + K_{s(\Delta\psi fd)} = 1{,}591 + 0.2804$

$= 1.8714$ pu torque/rad

The damping torque component due to $\Delta\psi_{fd}$ is

$K_{D(\Delta\psi fd)} = -0.3255(j\Delta\delta)$

Since $\Delta\omega_r = sD\delta/\omega_0 = j\omega\Delta\delta/\omega_0$,

$$K_{D(\Delta\psi)} = -\frac{0.325\omega_0}{\omega}\Delta\omega_r$$

With ω=10 rad/s, the damping torque coefficient is

$K_{D(\Delta\psi fd)} = -12.27$ pu torque/pu speed change

Usually, the point of interest lies in the performance of excitation system with moderate or high responses. For such excitation systems, we can make the following general observations regarding the effect of the AVR can be made.

- With K_5 positive, the effect of the AVR is to introduce a negative synchronizing torque and a positive damping torque component.
- The component K_5 is positive for low values of external system reactance and low generator outputs.
- With K_5 negative, the AVR action introduces a positive synchronizing torque component and a negative damping torque component. This effect is more pronounced as the exciter response increases.
- For high values of external system reactance and high generator outputs K_5 is negative. In practice, the situation where K_5 is negative is commonly encountered. For such cases, a high response exciter is beneficial in increasing synchronizing torque. However, in so doing it introduces negative damping. Thus conflicting requirements arise with regard to exciter response so that it results in sufficient synchronizing and damping torque components for the expected range of system operating conditions. This may not always be possible. It may be necessary to use a high response exciter to provide the required synchronizing torque and transient stability performance. With a very high external system reactance, even with low exciter response the net damping torque coefficient may be negative.

CHAPTER-3

CONVENTIONAL POWER SYSTEM STABILIZER

3.1 Components of a conventional PSS

The parameters of the PSS and other elements of the excitation system are chosen to enhance the overall system stability. Specifically, the following are the objectives of excitation control design:

- Enhancement of system transient stability.
- Maximization of damping of the local plant mode as well as inter-area mode oscillation without compromising the stability of other modes.
- Prevention of adverse affects on system performance during rajor system that cause large frequency excursions.
- Minimization of the consequences of excitation system malfunctions because of component failures.

The procedure used for meeting the above objectives is illustrated by considering a thyristor excitation system. The input to the PSS may be either the shaft speed deviation $(\Delta\omega_r)$ or the equivalent rotor speed deviation$(\Delta\omega_{eq})$. The terminal voltage transducer circuitry is represented by time constants necessary for filtering the rectified terminal voltage waveform. These can usually be reduced to a single time constant (T_R) in the range of 0.01 to 0.02 seconds. Others time constants through to the exciter output, including any associated with the exciter itself, are negligible and the main path can be represented simply by the gain K_A.

The following is a description of the considerations and procedures used for selection of the various parameters.

Exciter Gain:

A High value K_A is desirable from the view point of transient stability. A suitable value of K_A is about 200.

Phase-lead Compensation:

To damp rotor oscillations, the PSS produce a component of electrical torque in phase with rotor speed deviation. This required phase-lead circuits to be used to compensate for the lag

between the exciter input (i.e., PSS outpt) and the resulting electrical torque. If the degree of phase compensation required a small, a single first-order block may be used.

The PSS is often required to enhance damping of either a local plant mode or an inter area mode of oscillation. While this mode receives special attention, the phase compensation should be designed so that the PSS contributes to damping over a wide range of frequency covering both inter-area and local modes of oscillation.

The first step in determining the phase compensation is to computer the frequency response between the exciter input and the generator electrical torque. In computing this response, however, the generator speed and rotor angle should remain constant. This is because when the excitation of a generator is modulated, the resulting change in electrical torque causes variations in rotor speed and angle that in turn affect the electrical torque. As the point of interest lies only in the phase characteristic between exciter input and electrical torque, the feedback through rotor angle variation should be eliminated by holding the speed constant. Therefore, the phase characteristic as function of frequency is obtained with a large inertia assumed for the machine under consideration (say 100 times the actual inertia). This ensures that the speed and angle do not change over the frequency range of importance for stabilizer design. (0.1 to 3 Hz).

The phase characteristic to be compensated varies to some extent with system conditions. Therefore, a characteristic acceptable for different system conditions is selected. Generally, Slight under compensation is preferable to overcompensation so that the PSS does not contribute to the negative synchronizing torque component. An under compensation by about 10^0 over the entire frequency range of interest provides the required degree of tolerance to allow for uncertainties in machine and system modeling.

Stabilizing Signal Washout:

The signal washout is a high-pass filter that prevents steady changes in speed from modifying the field voltage. The value of washout time constant T_w should be high enough to allow signal associated with oscillations in rotor speed to pass unchanged.

From the viewpoint of the "washout function, "The main considerations are that it should be long enough to pass stabilizing signals at the frequencies of interest relatively unchanged, but

not so long that it leads to undesirable generator voltage excursions as a result of stabilizer action during system-islanding conditions. Ideally, the stabilizer should not respond to system-wide frequency variations.

For local mode oscillations in the range of 0.8 to 2.0 Hz, a washout of 1.5 seconds is satisfactory. From the viewpoint of low-frequency oscillations, a washout time constant of 10 seconds or higher desirable, since-time constant results in significant phase lead at low frequencies. Unless this compensated for elsewhere, it will reduce the synchronizing torque component at inter-area frequency.

Stabilizer Gain

The stabilizer gain K_{STAB} has an important effect on damping of rotor oscillations. The value of the gain is chosen by examining the effect for a wide range of value. The damping increases with an increase in stabilizer gain up to certain point beyond which further increase in gain result in a decrease in damping. Ideally, the stabilizer gain should be set at a value corresponding to maximum damping. However, the gain is often limited by other considerations.

Stabilizer gain is normally set to a value that results in as high a damping the critical system mode (s) as practical without compromising the stability of other system modes or causing excessive amplification of signal noise.

Check on selected settings:

The final stage in stabilizer design involves the evaluation of its effect on the overall system performance. First, the effect of the stabilizer on various modes of system oscillations is determined over a wide range of system conditions by using a small- signal stability program. This includes analysis of the effect of the PSS on local plant modes, inter-area modes, control modes. In particular, it is important to ensure that there are no adverse interactions with the controls of other nearby generating units and devices.

The excitation control systems, designed as described above, provide effective decentralized controllers for the damping of electromechanical oscillations in power systems. Generally, the resulting design is much more robust that can be achieved through use of other methods such as pole placement techniques and multivariable state space techniques. The overall

approach is used on acknowledge of the physical aspect the power system stabilization problem. The method used for establishing the phase characteristics of the PSS is simple and required only the dynamic characteristics the concerned machines to be modeled in details. Detailed analysis of the performance of the power system is used to establish other parameters and to ensure adequacy of the overall performance of the excitation control. The result is a control that enhances the overall stability of the system under different operating conditions. Since the PSS is turned to increase the damping torque component for a wide range of frequencies it contributes to the damping of all system modes in which the respective generator has a high participation. This includes any new mode that may emerge as a result changing system conditions. It is possible to satisfy the requirements for a wide range of system conditions with fixed parameters; there has been little incentive to date to consider an adaptive control system.

3.2 State space model of PSS

The basic function of Power System Stabilizer (PSS) is to add damping to the generator rotor oscillations by controlling its excitation using auxiliary stabilizing signal(s).To provide damping, the stabilizer must produce a component of electrical torque in phase with the rotor speed deviations. Since the purpose of a PSS is to introduce a damping torque component, a logical signal to use for controlling generator excitation is the speed deviation $\Delta\omega_{r.}$

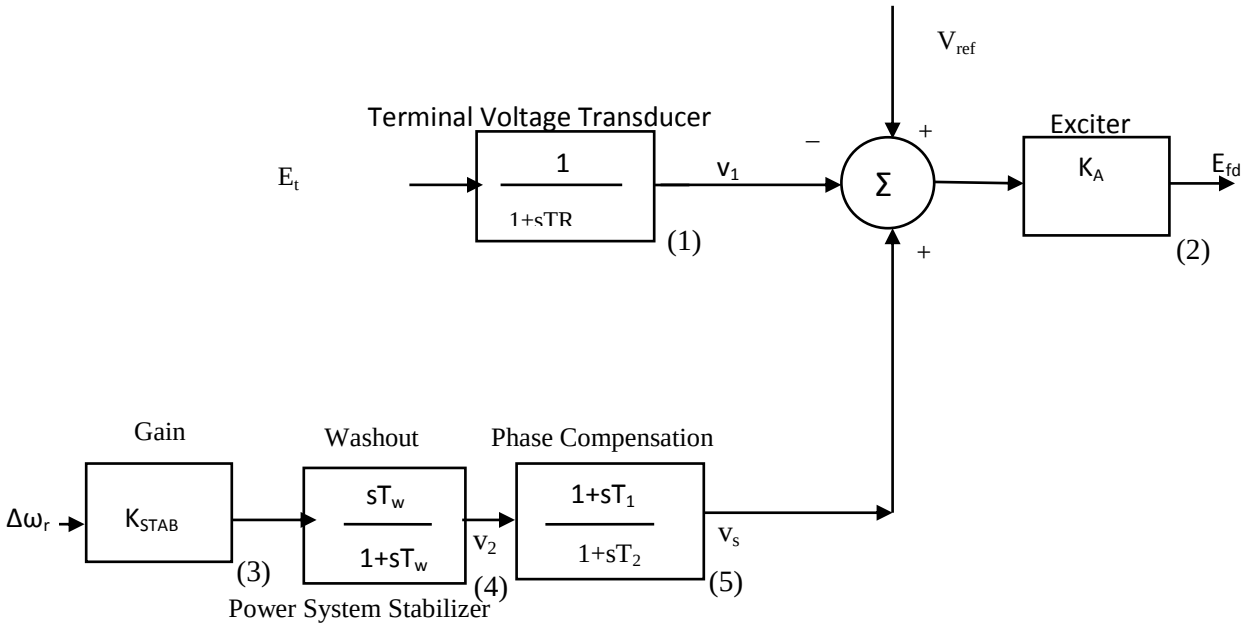

Figure 3.1: Thyristor excitation system with AVR and PSS

Figure 3.1 shows the block diagram of the excitation system, including the AVR and PSS. Since we are concerned with small signal performance, stabilizer output limits and exciter output limits are not shown in the figure.

The PSS representation in Figure 3.1 consists of the blocks : a phase compensation block, signal washout block and a gain block.

The phase compensation block provides the appropriate phase-lead characteristic to compensate for the phase lag between the exciter input and the generator electrical (air-gap) torque. The figure showed a single first order block. In practice, two or more first-order block may be used to achieve the desired phase compensation.

Normally, the frequency range of interest is 0.1 to 2.0 Hz, and the phase -lead network should provide compensation over this entire frequency range. The phase characteristic to be compensated changes with system conditions; therefore, a compromise is made and a characteristic is desirable so that the PSS, in addition to significantly increasing the damping torque, results in a slight increase of the synchronizing torque.

The signal washout block serves as a high-pass filter , with time constant Tw high enough to allow signals associated with oscillations in ωr to pass unchanged. Without it, steady changes in speed would modify the terminal voltage. It allows the PSS to respond only to changes in speed. From the viewpoint of the washout function, the value of Tw is not critical and may be in the range of 1 to 20 seconds. The main consideration is that it be long enough to pass stabilizing signals at the frequencies of interest unchanged, but not so long that it leads to undesirable generator voltage excursions during system-islanding conditions.

The stabilizer gain K_{STAB} determines the amount of damping introduced by the PSS. Ideally, the gain should be set at a value corresponding to maximum damping, however it is often limited by other considerations.

If the exciters transfer function $G_{ex(s)}$ and the generator transfer function between ΔE_{fd} and ΔT_e were pure gains, a direct feedback of $\Delta\omega r$ would result in a damping torque component. However, in practice both the generator and the exciter exhibit frequency dependent gain and phase characteristics. Therefore the PSS transfer function, $G_{PSS(s)}$, should have appropriate phase

compensation circuits to compensate for the phase lag between the exciter input and the electrical torque. In the ideal case, with the phase characteristic of $G_{Pss(s)}$ being an exact inverse of the exciter and generator phase characteristic to be compensated, the PSS would result in a pure damping torque at all oscillating frequencies.

Example: Principle of PSS can be illustrated by considering the example of last chapter used for examining the effect of the excitation system. the parameters of the system as before are

K_1=1.591 K_2=1.5 K_3=0.333 K_D=0.0 H=3.0

T_3=1.91 K_5= - 0.12 K_6 = 0.3 $G_{ex}(s) = K_A = 200$

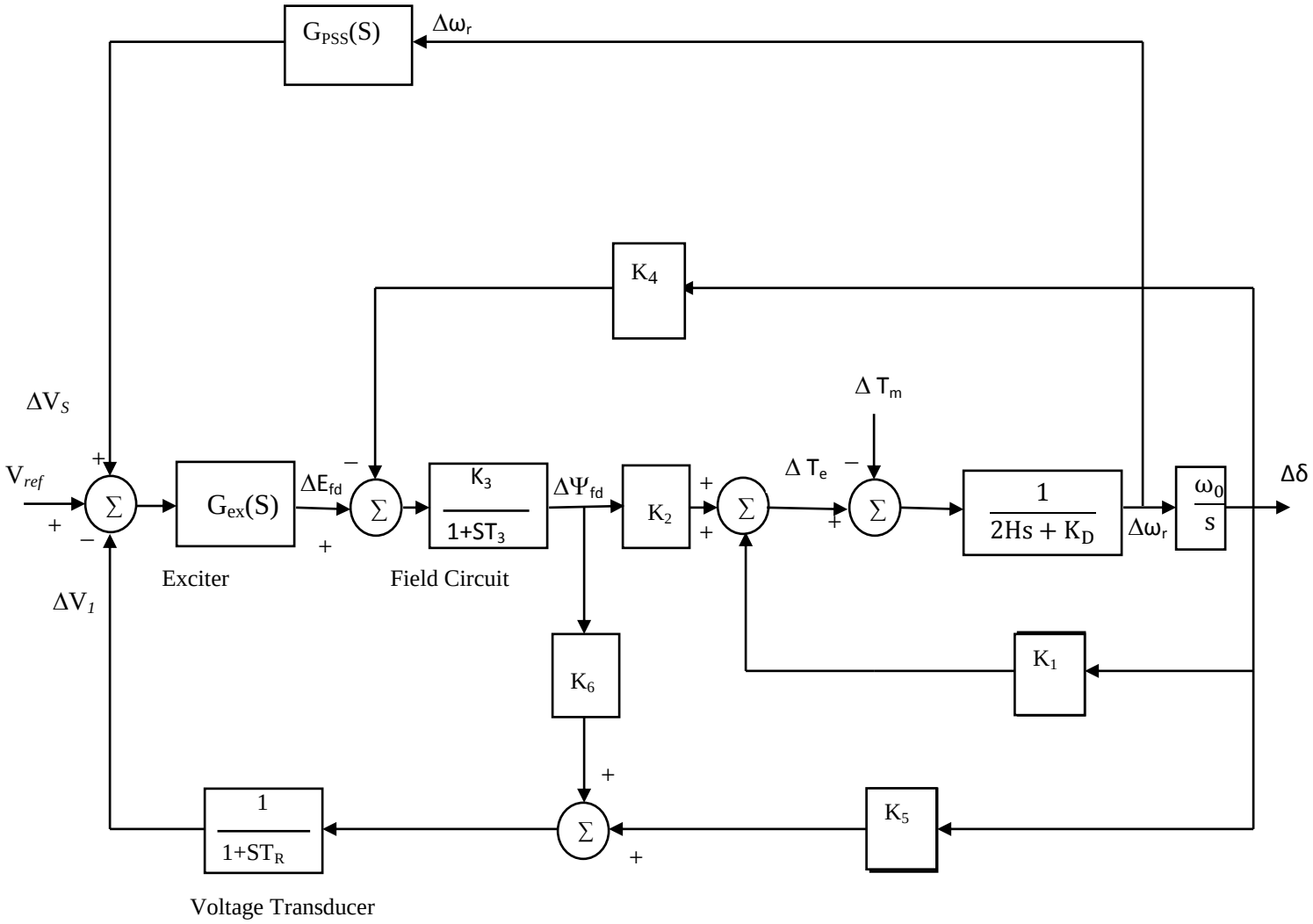

Figure 3.2 : Composite Block Diagram Representation of SMIB System with AVR and PSS

Since T_R is very small in comparison to T_3, its effect is neglected in examining the PSS performance.

From the block diagram of figure 3.2 with TR neglected, $\Delta\psi_{fd}$ due to PSS is given by

$$\Delta\psi_{fd} = \frac{K_3 K_A}{1 + sT_3}\left(-K_6\Delta\psi_{fd} + \Delta v_s\right)$$

therefore

$$\frac{\Delta\psi_{fd}}{\Delta v_s} = \frac{K_3 K_A}{sT_3 + 1 + K_3 K_6 K_A}$$

$$= \frac{0.333 \times 200}{1.91s + 1 + 0.333 \times 0.3 \times 200}$$

$$= \frac{66.66}{1.91s + 21}$$

Let us examine the PSS phase compensation required to produce damping torque at a rotor oscillation frequency of 10 rad/s. With s = jω = j10,

$$\frac{\Delta\psi_{fd}}{\Delta v_s} = \frac{66.66}{21 + j1.91}$$

$\Delta Tpss = \Delta T_{e\ due}$ to PSS = K2 ($\Delta\psi_{fd\ due\ to\ PSS}$)

Therefore, at frequency of 10 rad/s.

$$\frac{\Delta T_{PSS}}{\Delta v_s} = K_2\left(\frac{66.66}{21 + j19.1}\right)$$

$$= \frac{1.5 \times 66.66}{21 + j\,19.1}$$

$$= 3.522 \angle -42.3^0$$

If ΔT_{pss} has to be in phase with $\Delta\omega_r$ (i.e., a purely damping torque), the $\Delta\omega_r$ signal should be processed through a phase-lead network so that the signal is advanced by $\theta = 42.3^0$ at a frequency of oscillation of 10 rad/s. The amount of damping introduced depends on the gain of PSS transfer function at that frequency. Therefore,

$$\Delta T_{pss} = (\text{gain of PSS at } \omega = 10)\ (3.522)(\Delta\omega_r)$$

With the phase-lead network compensating exactly for the phase lag between ΔT_e and ΔV_s, the above compensation is purely damping.

The damping torque coefficient due to PSS at $\omega = 10$ rad/s is equal to

$$K_D \text{ (PSS)} = \text{(gain of PSS) (3.522)}$$

Therefore, the net K_D including the effect of AVR and PSS is

$$K_D = K_D \text{ (AVR)} + K_D \text{ (PSS)}$$

If the phase-lead network provides more compensation that the phase lag between ΔT_e and $\Delta v_s$the PSS introduce, in addition to a damping component of torque, a negative synchronizing torque component. Conversely, with under compensation positive synchronizing torque component is introduced. Usually, the PSS is required to contribute to the damping of rotor oscillations over a range of frequencies, rather than a single frequency.

3.3 System State-Space model including PSS

From block 4 Figure 3.1, using perturbed values, we have

$$\Delta v_2 = \frac{pT_w}{1 + pT_w}(K_{STAB}\Delta\omega_r)$$

Hence

$$p\Delta v_2 = K_{STAB}p\omega_r - \frac{1}{T_w}\Delta v_2$$

Substituting for p$\Delta\omega_r$ given by Equation 2.28, we obtain the following express for pΔv_2in terms of the state variables:

$$p\Delta v_2 = K_{STAB}\left[a_{11}\Delta\omega_r \ + \ a_{12}\Delta\delta + \ a_{13}\Delta\psi_{fd} + \frac{1}{2H}\Delta T_m\right] - \ \frac{1}{T_w}\Delta v_2$$

$$= \ a_{51}\Delta\omega_r + \ a_{52}\Delta\delta + a_{53}\Delta\,\psi_{fd} + \ a_{55}\Delta v_2 \ + \ \frac{K_{STAB}}{2H}\Delta T_m$$

where

$$a_{51} = K_{STAB}a_{11} \qquad a_{52} = K_{STAB}a_{12}$$

$$a_{53} = K_{STAB}a_{13}$$

$$a_{55} = \frac{-1}{T_w}$$

Since $p\Delta v_2$ is not function of Δv_1 andΔv_3, $a_{54} = a_{56} = 0$

From block 5 of 3.1,

$$\Delta v_s = \ \Delta v_2\left(\frac{1 + pT_1}{1 + pT_2}\right)$$

Hence

$$p\Delta v_s = \ \frac{T_1}{T_2}p\Delta v_2 + \ \frac{1}{T_2} - \frac{1}{T_2}\Delta v_s$$

Substitution for $p\Delta v_2$given by Equation 5.1 yields

$$p\Delta v_s = \ a_{61}\Delta\omega a_{62}\Delta\delta + a_{63}\Delta\psi_{fd} +$$

$$a_{64}\Delta v_1 + a_{65}\Delta v_2 + a_{66}\Delta v_s + \frac{T_1}{T_2}\,\frac{K_{STAB}}{2H}\Delta T_m$$

Where

$$a_{61} = \frac{T_1}{T_2}a_{51}$$

$$a_{62} = \frac{T_1}{T_2}a_{52}$$

$$a_{63} = \frac{T_1}{T_2} a_{53}$$

$$a_{64} = \frac{T_1}{T_2} a_{55} + \frac{1}{T_2}$$

$$a_{66} = \frac{-1}{T_2}$$

From block 2 of Figure 5.2

$\Delta E_{fd} = K_A (\Delta v_s - \Delta v_1)$

The field circuit equation, with PSS included, becomes

$$p\Delta\psi_{fd} = a_{32}\Delta\delta + a_{33}\Delta\psi_{fd} + a_{34}\Delta v_1 + a_{36}\Delta v_s$$

Where

$$a_{36} = \frac{\omega_0 R_{fd}}{L_{ads}} K_A$$

The complete state-space model, including the PSS, has the following form (with $\Delta T_m = 0$):

$$\begin{bmatrix} \Delta\dot{\omega}_r \\ \Delta\dot{\delta} \\ \Delta\dot{\psi}_{fd} \\ \Delta\dot{v}_1 \\ \Delta\dot{v}_2 \\ \Delta\dot{v}_s \end{bmatrix} = \begin{bmatrix} a_{11} & a_{12} & a_{13} & 0 & 0 & 0 \\ a_{21} & 0 & 0 & 0 & 0 & 0 \\ 0 & a_{32} & a_{33} & a_{34} & 0 & a_{36} \\ 0 & a_{42} & a_{43} & a_{44} & 0 & 0 \\ a_{51} & a_{52} & a_{53} & 0 & a_{55} & 0 \\ a_{61} & a_{62} & a_{63} & 0 & a_{65} & a_{66} \end{bmatrix} \begin{bmatrix} \Delta\omega_r \\ \Delta\delta \\ \Delta\psi_{fd} \\ \Delta v_1 \\ \Delta v_2 \\ \Delta v_s \end{bmatrix}$$

Block 4 of fig 3.1 may be considered to be made up to two blocks:

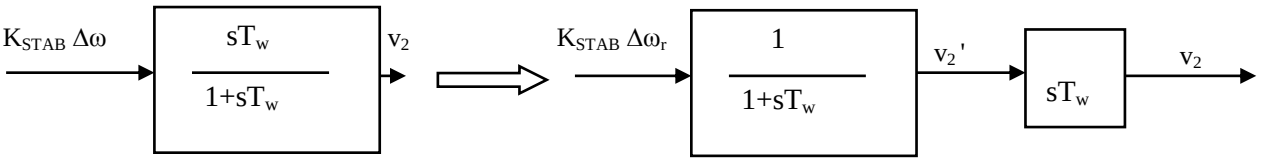

(4) (4 A) (4 B)

In this case, $\Delta v_2'$ becomes the state variables, with

$$p\Delta v_2' = \frac{1}{T_w}\left(K_{STAB}\Delta\omega_r - \Delta v_2'\right)$$

and the output Δv_2 of the block is given by

$$\Delta v_2 = T_w p\Delta v_2'$$
$$= K_{STAB}\Delta\omega_r - \Delta v_2'$$

The advantage of this approach is that the expression for the derivative of the input variable to the block is not required. This is important is situations where the input is not a state variable, in which case the expression for its derivative is not readily available. Similarly, block 5 may be treated as follows:

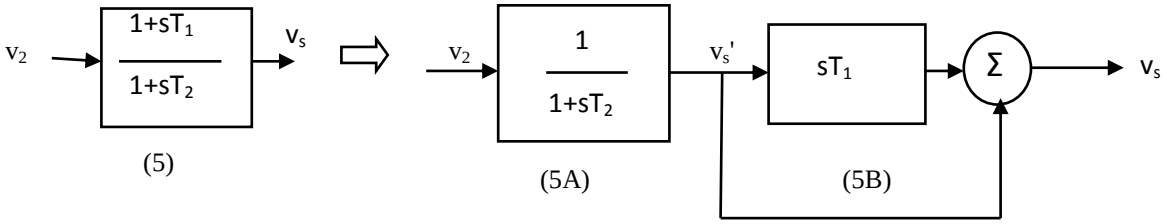

In this case $v_s'$is the state variable, with

$$p\Delta v_s' = \frac{1}{T_2}\left(\Delta v_2 - \Delta v_s'\right)$$

and the output Δv_s is given by

$$\Delta v_s = T_1 p\Delta v_s' + \Delta v_s'$$

$$= \frac{T_1}{T_2}\Delta v_2 + \left(1 - \frac{1}{T_2}\right)\Delta v_s'$$

CHAPTER- 4

FUZZY LOGIC BASED POWER SYSTEM STABILIZER

4.1 Basic Concept of Fuzzy Logic System

Fuzzy logic, as its name suggests, is the logic underlying modes of reasoning which are approximate rather than exact. Fuzzy Logic Controllers (FLC) are very useful when an exact mathematical model of the plant is not available; however, experienced human operators are available for providing qualitative rules to control the system. Fuzzy logic, which is the logic on which fuzzy logic control is based, is much closer in spirit to human thinking and natural language than the traditional logic systems. Basically, it provides an effective mean of capturing the approximate, inexact nature of our knowledge about the real world. Viewed in this perspective, the essential part of the FLC is a set of linguistic control rules related by dual concepts of fuzzy implication and the compositional rule of inference.

The fuzzy logic is capable to handle approximate information in a systematic way and therefore it is suited for controlling non- linear systems and for modeling complex systems where an inexact model exists or systems where ambiguity or vagueness is common. The importance of fuzzy logic derives from the fact that most modes of human reasoning and especially common sense reasoning are approximate in nature. In doing so, the fuzzy logic approach allows the designer to handle efficiently very complex closed-loop control problems. There are many artificial intelligence techniques that have been employed in modern power systems, but fuzzy logic has emerged as the powerful tool for solving challenging problems. As compared to the conventional controller, the fuzzy logic controller has some advantages such as:

- A simpler and faster methodology.
- It does not need any exact system mathematical model.
- It can handle nonlinearity of arbitrary complexity.

- It is based on the linguistic rules with an IF-THEN general structure, which is the basis of human logic.
- It is more robust than conventional nonlinear controllers.

4.2 Fuzzy Inference System

The fuzzy inference system or fuzzy system is a popular computing frame- work based on the concept of fuzzy set theory, fuzzy if-then rules, and fuzzy reasoning.

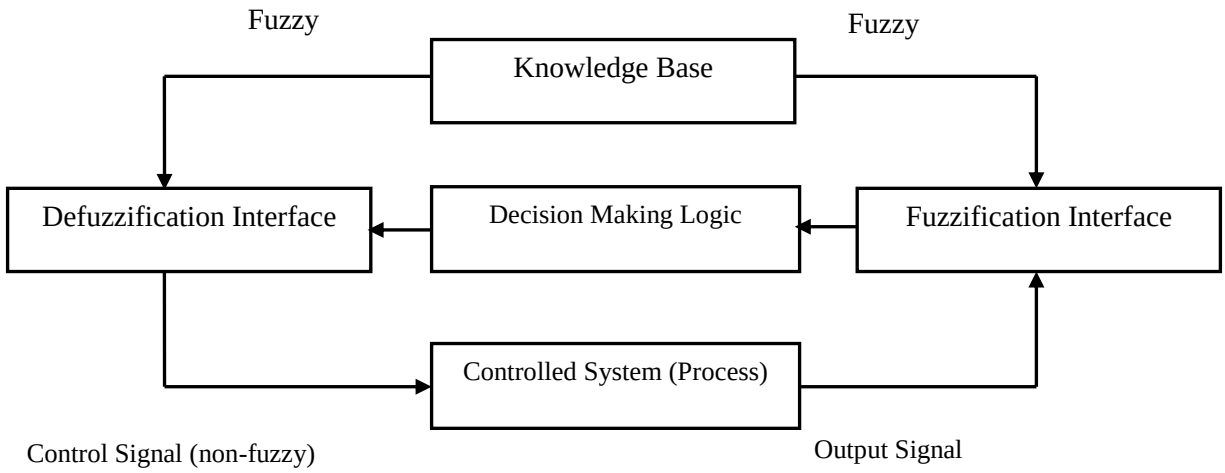

Figure 4.1: Block diagram of Fuzzy logic controller

The fuzzy inference system basically consists of a formulation of the mapping from a given input set to an output set using FL as shown in Figure 4.1. The mapping process provides the basis from which the inference or conclusion can be made. The basic structure of fuzzy inference system consists of three conceptual components: a rule base, which contains a selection of fuzzy rules; a data base, which defines the membership functions used in the fuzzy rules; and a reasoning mechanism which performs the inference procedure upon the rules and given facts to derive a reasonable output or conclusion. The fuzzy logic controller comprises four principle components: fuzzification interface, knowledge base, decision making logic, and defuzzification interface.

Fuzzification: In fuzzification, the values of input variables are measured i.e. it converts the input data into suitable linguistic values.

Knowledge base: The knowledge base consists of a database and linguistic control rule base. The database provides the necessary definitions, which are used to define the linguistic control rules and fuzzy data manipulation in an FLC. The rule base characterizes the control policy of domain experts by means of set of linguistic control rules.

Decision making logic: The decision making logic has the capability of stimulating human decision making based on fuzzy concepts.

Defuzzification: The defuzzification performs scale mapping, which converts the range of values of output variables into corresponding universe of discourse. If the output from the defuzzifier is a control action for a process, then the system is a non-fuzzy logic decision system. There are different techniques for defuzziffication such as maximum method, height
method, centroid method etc.

The basic inference process consists of the following five steps:

Step 1: Fuzzification of input variables.

Step2: Application of fuzzy operator (AND, OR, NOT) in the IF (antecedent) part of the rule.

Step3: Implication from the antecedent to the consequent THEN part of the rule.

Step4: Aggregation of the consequents across the rules.

Step5: Defuzzification.

4.3 Design of Fuzzy Logic Based PSS

The basic structure of the fuzzy logic controller is shown in Figure 4.2. Here the inputs to the fuzzy logic controller are the normalized values of error 'e' and change of error 'ce'. Normalization is done to limit the universe of discourse of the inputs between -1 to 1 such that the controller can be successfully operated within a wide range of input variation. Here 'K_e' and 'K_{ce}' are the normalization factors for error input and change of error input respectively. For this fuzzy logic controller design, the normalization factors are taken as constants. The output of the fuzzy logic

controller is then multiplied with a gain 'K_0' to give the appropriate control signal *'U'*. The output gain is also taken as a constant for this fuzzy logic controller.

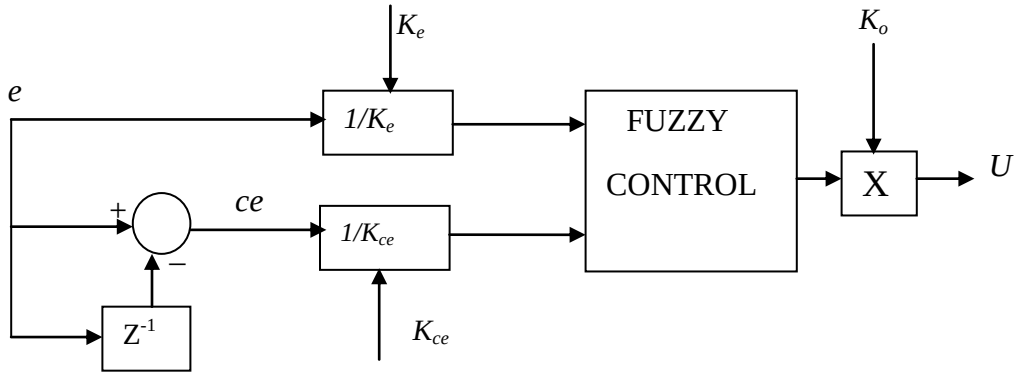

Figure 4.2 : Basic Structure of Fuzzy logic Controller

The fuzzy controller used in power system stabilizer is normally a two- input and a single-output component. The two inputs are change in angular speed ($\Delta\omega$) and rate of change of angular speed ($\Delta\dot{\omega}$) whereas output of fuzzy logic controller is a voltage signal.

Input /Output Variables:

The design starts with assigning the mapped variables inputs/output of the fuzzy logic controller. The first input variable to the FLC is the generator speed deviation and the second is acceleration. The output variable to the FLC is the voltage.

After choosing proper variables as input and output of fuzzy controller, it is required to decide on the linguistic variables. These variables transform the numerical values of the input of the fuzzy controller to fuzzy quantities. The number of linguistic variables describing the fuzzy subsets of a variable varies according to the application. Here seven linguistic variables for each of the input and output variables are used as described in Table 4.1. Figures 4.3 ,4.4 and 4.5 show the membership functions for fuzzy variables. The membership function maps the crisp values into fuzzy variables.

NB	NEGATIVE BIG
NM	NEGATIVE MEDIUM
NS	NEGATIVE SMALL
ZE	ZERO
PS	POSITIVE SMALL
PM	POSITIVE MEDIUM
PB	POSITIVE BIG

Table 4.1: Input and output linguistic variables

The triangular membership functions are used to define the degree of membership. Here for each input variable, seven labels are defined namely NB, NM, NS, ZE, PS, PM and PB. Each subset is associated with a triangular

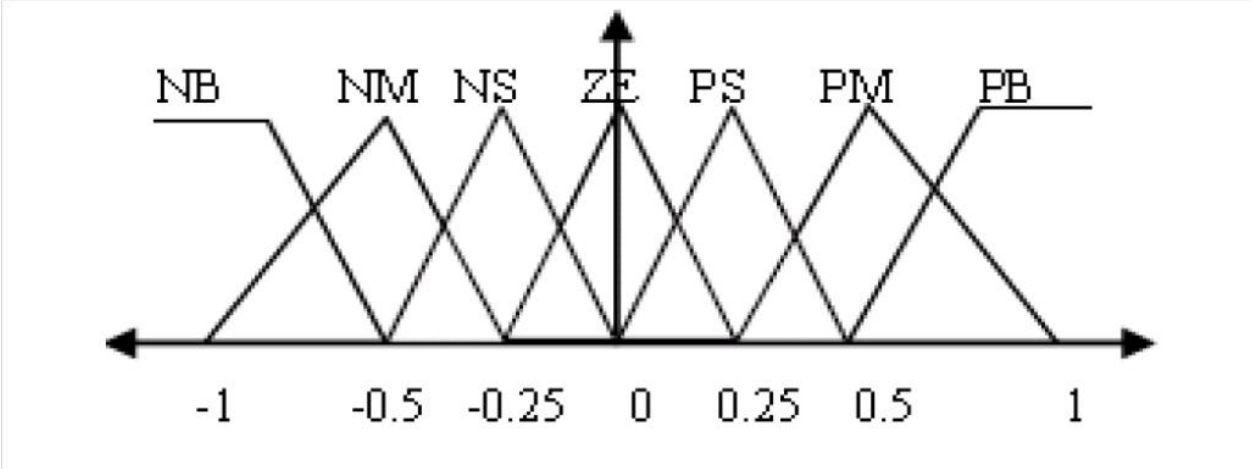

Figure 4.3: Membership function for speed deviation

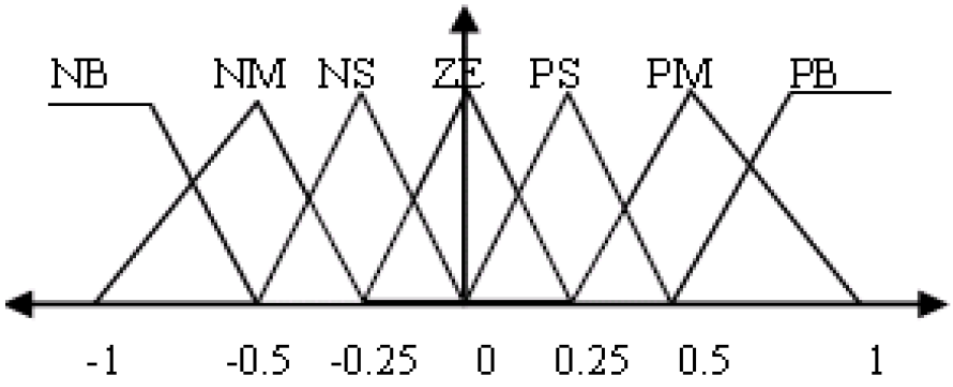

Figure 4.4: Membership function for acceleration

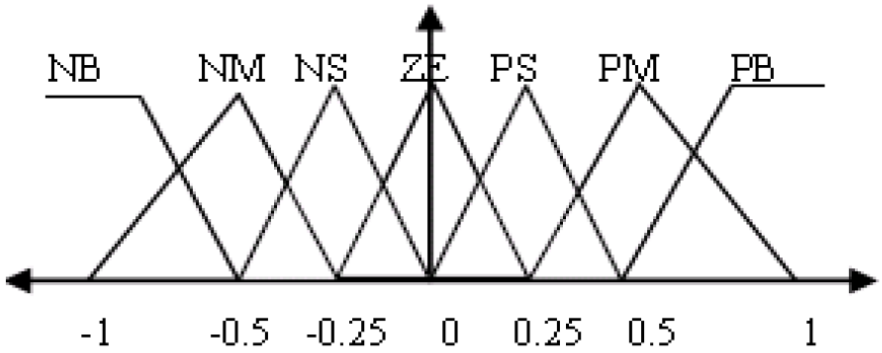

Figure 4.5: Membership function for voltage

Speed Deviation	***Acceleration***						
	NB	***NM***	***NS***	***ZE***	***PS***	***PM***	***PB***
NB	NB	NB	NB	NB	NM	NM	NS
NM	NB	NM	NM	NM	NS	NS	ZE
NS	NM	NM	NS	NS	ZE	ZE	PS
ZE	NM	NS	NS	ZE	PS	PS	PM
PS	NS	ZE	ZE	PS	PS	PM	PM
PM	ZE	PS	PS	PM	PM	PM	PB
PB	PS	PM	PM	PB	PB	PB	PB

Table 4.2 : Decision Table

The variables are normalized by multiplying with respective gains *Ke ; Kce ;* K_0 so that their values lie between -1 and +1. The membership function for speed deviation, acceleration and voltage are shown in Figure 4.4, Figure 4.5 and Figure 4.6 respectively.

Knowledge base involves defining the rules represented as IF - THEN rules statements governing the relationship between input and output variables in terms of membership functions. In this stage the input variables speed deviation and acceleration are processed by the inference engine that executes 7 x 7 rules represented in rule Table 4.2. Each entity shown in Table 4.7 represent a rule. The antecedent of each rule conjuncts speed deviation ($\Delta\omega$) and acceleration (a) fuzzy set values. The knowledge required to generate the fuzzy rules can be derived from an offine simulation. Some knowledge can be based on the understanding of the behavior of the dynamic system under control. For monotonic systems, a symmetrical rule table is very appropriate, although sometimes it may need slight adjustment based on the behavior of the specific system. If the system dynamics are not known or are highly nonlinear, trial and error procedures and experience play an important role in defining the rules.

The typical rules are having the following structure:

Rule 1**:** If speed deviation is NB (Negative Big) AND acceleration is also NB (Negative Big) then voltage (output of fuzzy PSS) is NB (Negative Big).

Rule 2**:** If speed deviation is NB (Negative Big) AND acceleration is NM (Negative Medium) then voltage (output of fuzzy PSS) is NB (Negative Big).

The fig.4.6 shows the rules for the fuzzy work. Each of the 49 control rules represents the desired controller response to a particular situation.

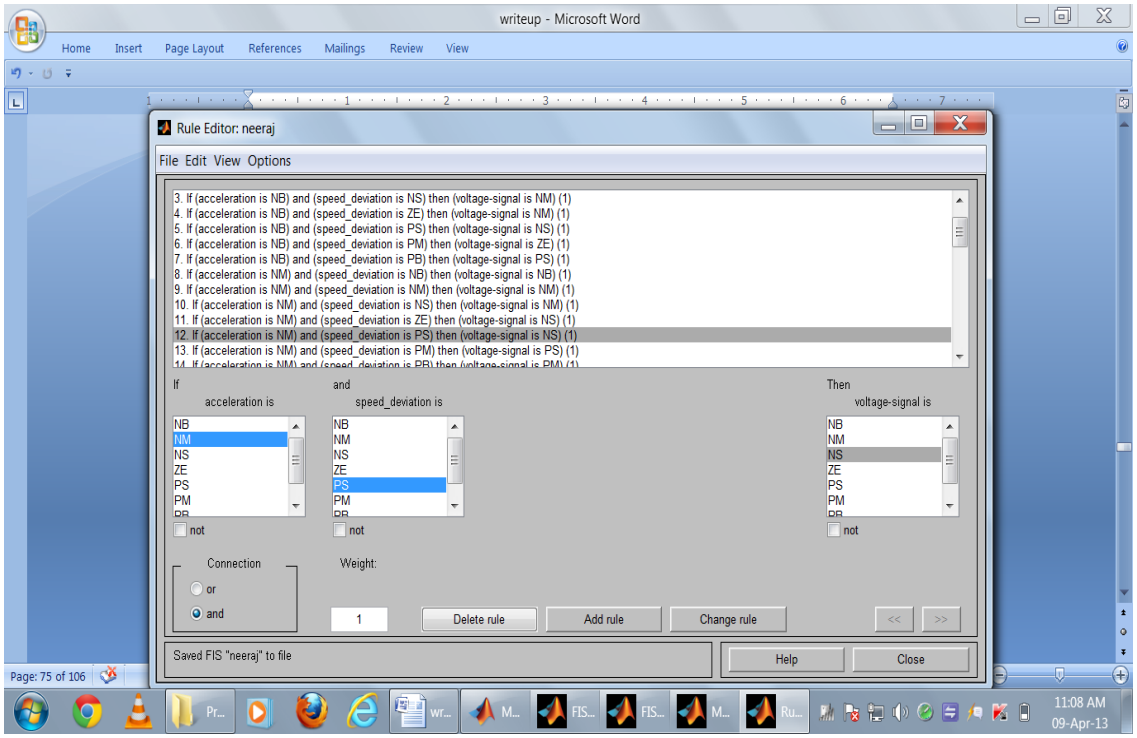

Figure 4.6 : Rule Editor

The procedure for calculating the crisp output of the Fuzzy Logic Controller (FLC) for some values of input variables is based on the following three steps.

Step 1: Determination of Degree of Firing (DOF) of the Rules

The DOF of the rule consequent is a scalar value which equals the mini mum of two antecedent membership degrees. For example if $\Delta\omega$ is PS with a membership degree of 0.6 and Δa is PM with a membership degree of 0.4 then the degree of firing of this rule is 0.4.

Step2: Inference Mechanism

The inference mechanism consists of two processes called fuzzy implication and aggregation. The degree of firing of a rule interacts with its consequent to provide the output of the rule, which is a fuzzy subset. The formulation used to determine how the DOF and the consequent fuzzy set interact to form the rule output is called a fuzzy implication. In fuzzy logic control the most commonly used method for inferring the rule output is Mamdani method.

Step3: Defuzzification

To obtain a crisp output value from the fuzzy set obtained in the previous step a mechanism called defuzzification is used. The output U is defuzzified according to the membership functions shown in fig. 4.5.Center of gravity (COA) or centroid method is used to calculate the final fuzzy value. Defuzzification using COA method means that the crisp output of U is obtained by using the centre of gravity, in which crisp U variable is taken to be the geometric centre of the output fuzzy variable value area $\mu_{out}(U)$ where $\mu_{out}(U)$ is formed by taking the union of all the contributions of rules with the degree of fulfillment greater than zero.

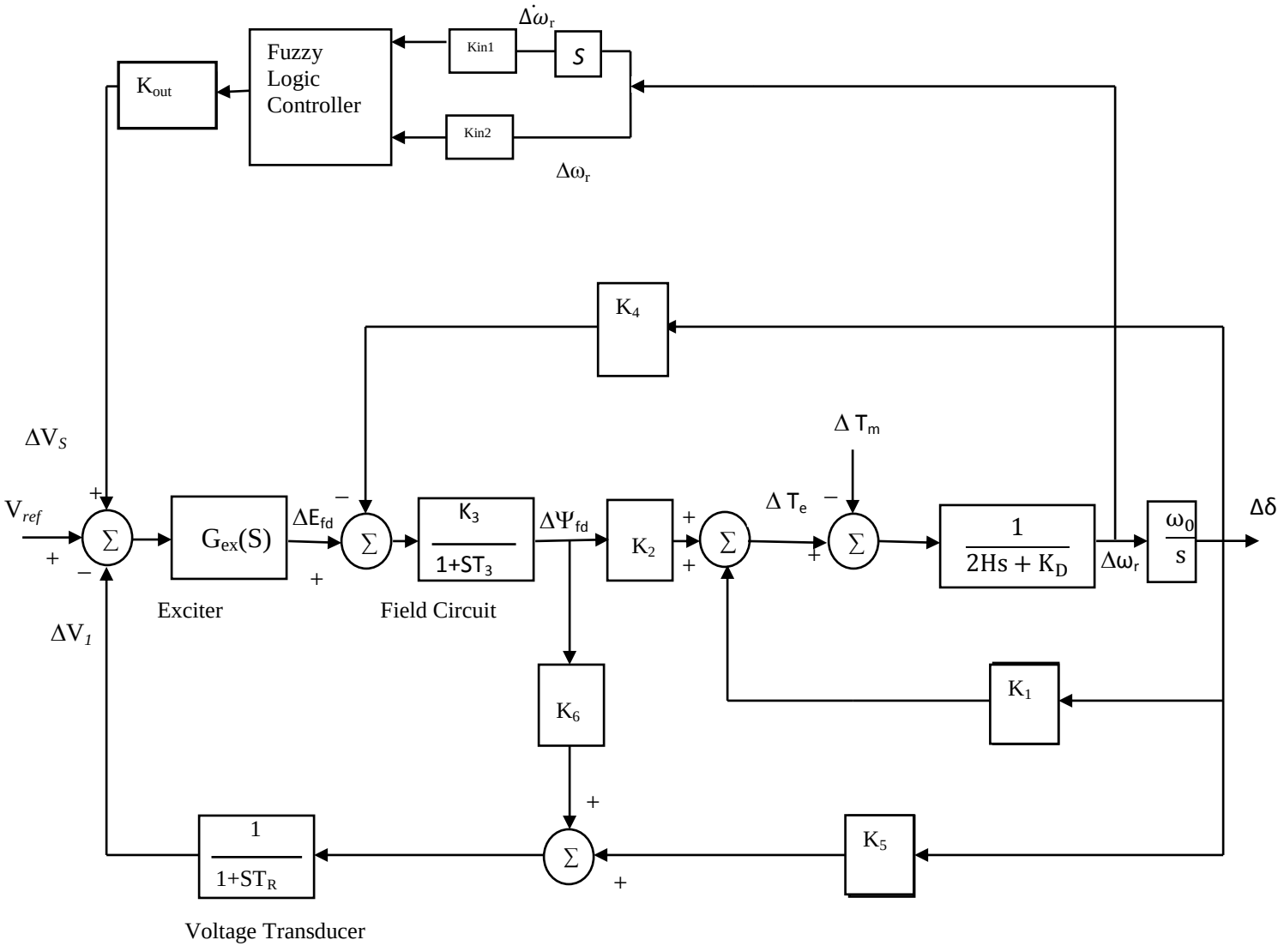

Figure 4.7 : Block Diagram Representation with Fuzzy Controller

After replacing the conventional PSS block by fuzzy controller block, the representation of fuzzy logic controller implemented on single machine infinite bus system can be shown in the Fig. 4.7. The fuzzy module has two inputs namely the angular velocity and its derivative i.e. angular acceleration and output parameter as voltage. These are normalized by gains K_{in1}, K_{in2} and K_{out} respectively to match the range on which the membership functions are defined. Parameters K_{in1}, K_{in2} and K_{out} are tuned to give the desired response.

CHAPTER- 5

CASE STUDY AND RESULTS

5.1: System under Consideration

In this chapter, simulation results using MATLAB / SIMULINK for both types of power system stabilizers (conventional and fuzzy based) are shown. The performance of the proposed model is tested on Single Machine Infinite Bus System (SMIB) as shown in Figure 5.1. The system data for modeling are given in Annexure 'A'. Then the performance of SMIB system has been studied without excitation system, with excitation system only, with conventional PSS (lead-lag) and with fuzzy logic based PSS by using the K constants.

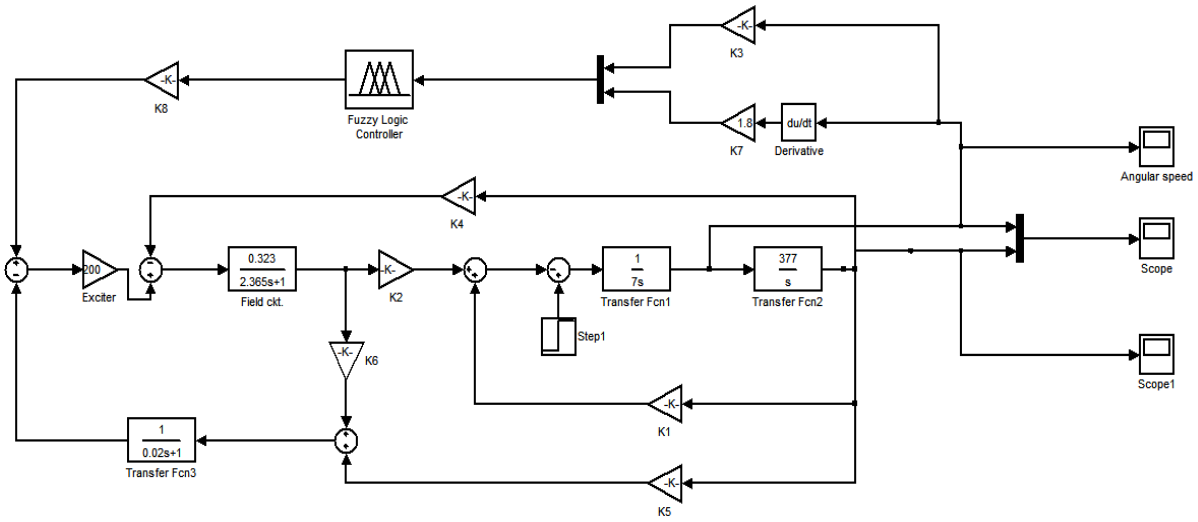

Figure 5.1: Test system (SMIB) for FPSS

At the end of the topic comparisons have been made between conventional PSS and fuzzy logic based PSS and accordingly arrived on the conclusions.

5.2 Results without AVR

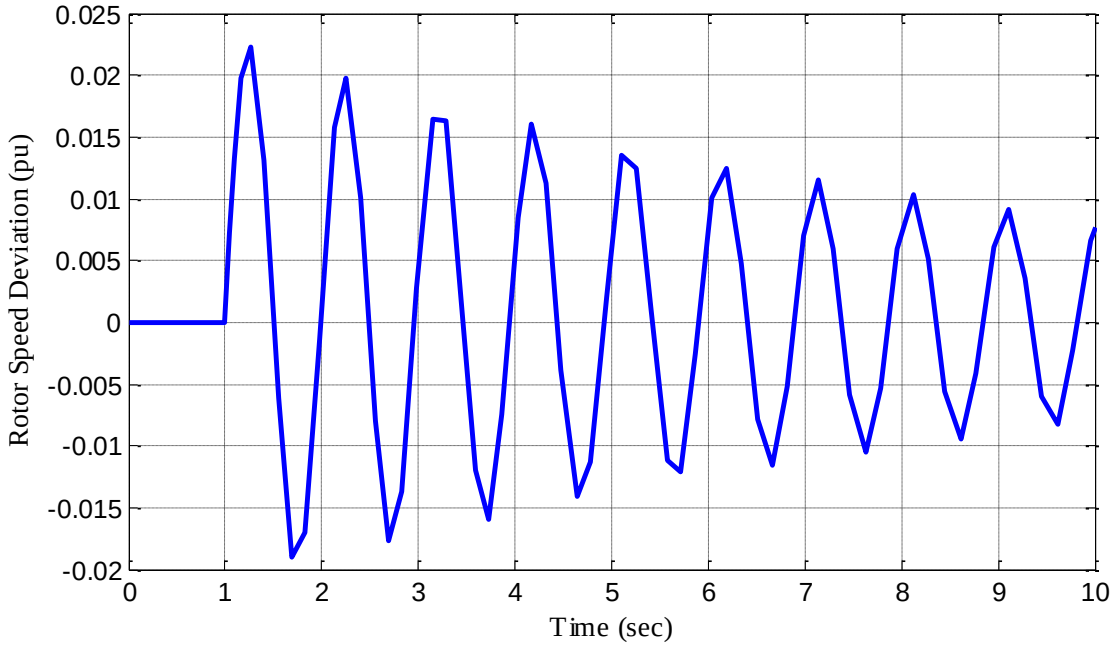

Figure 5.2: Variation of angular speed without AVR

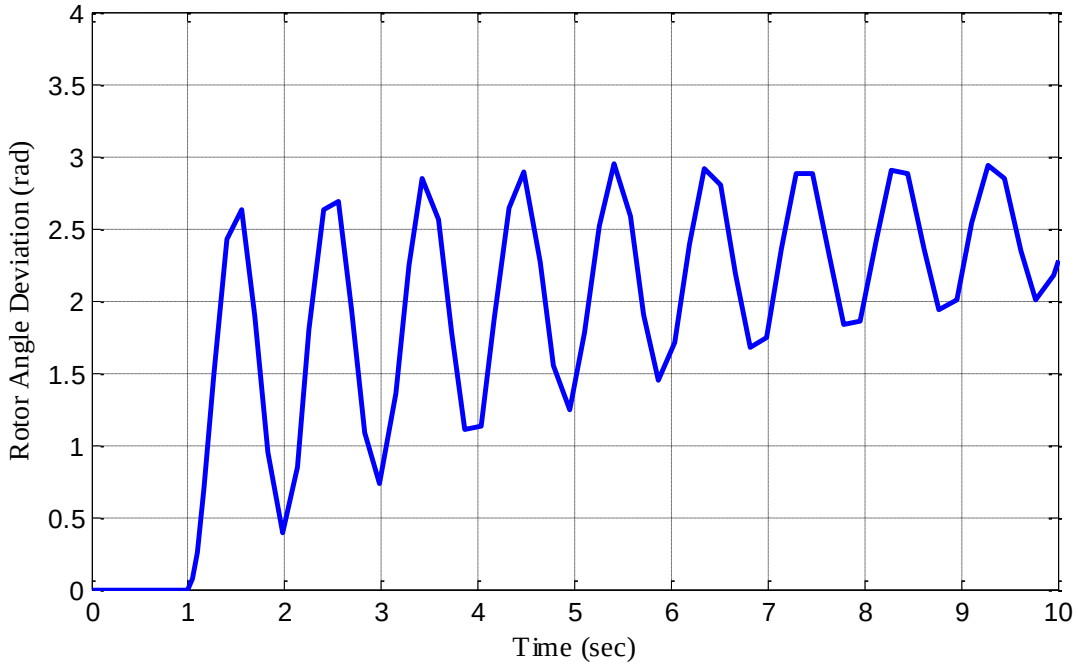

Figure 5.3: Variation of angular position without AVR

5.3 Results with AVR only

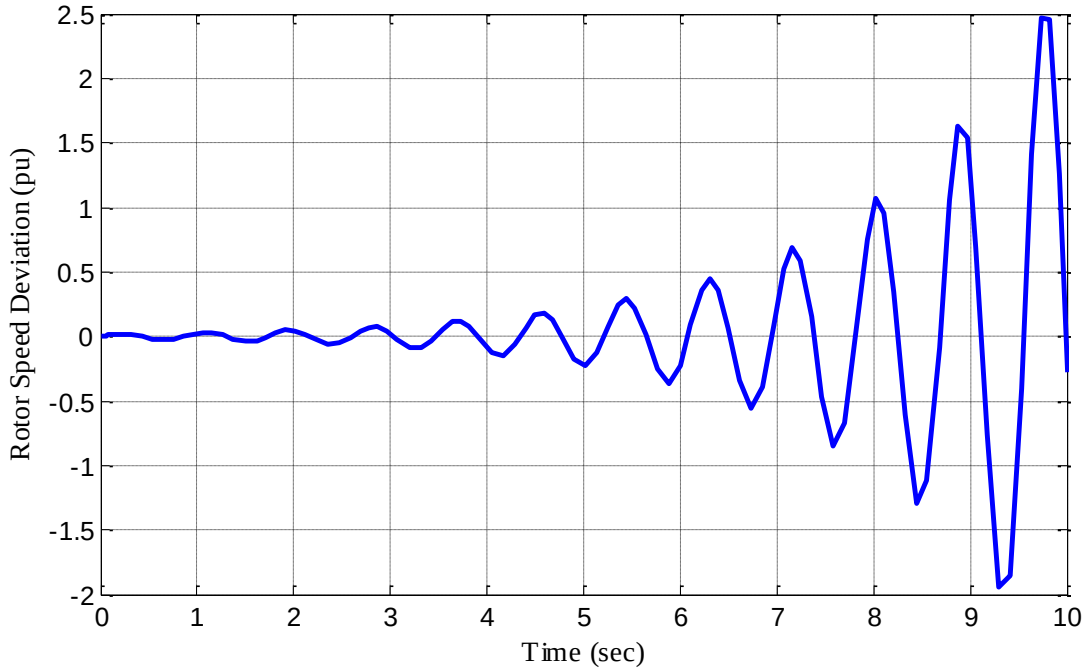

Figure 5.4: Variation of angular speed with AVR only

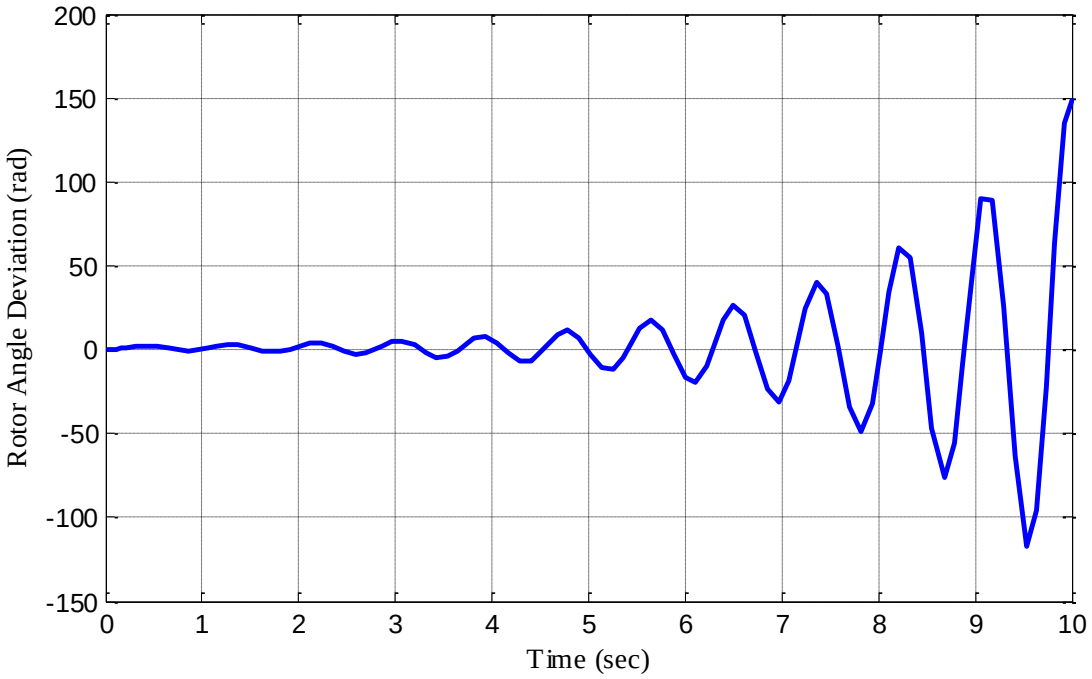

Figure 5.5: Variation of angular position with AVR only

5.4 Results with Conventional PSS

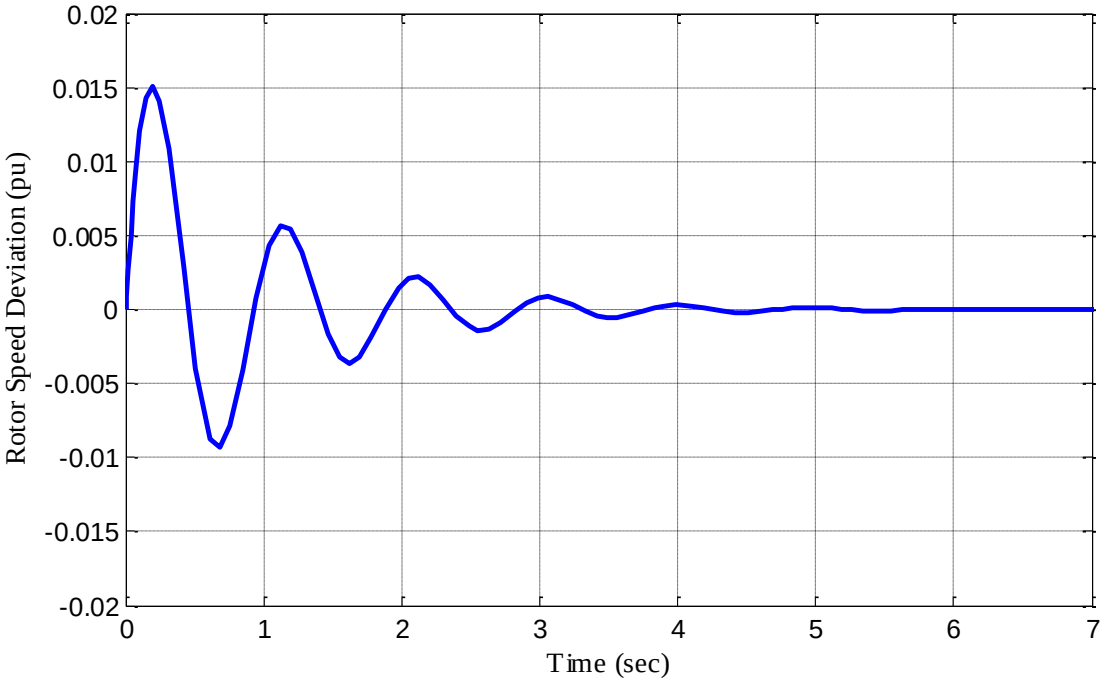

Figure 5.6: Variation of angular speed with CPSS (P = 0.9)

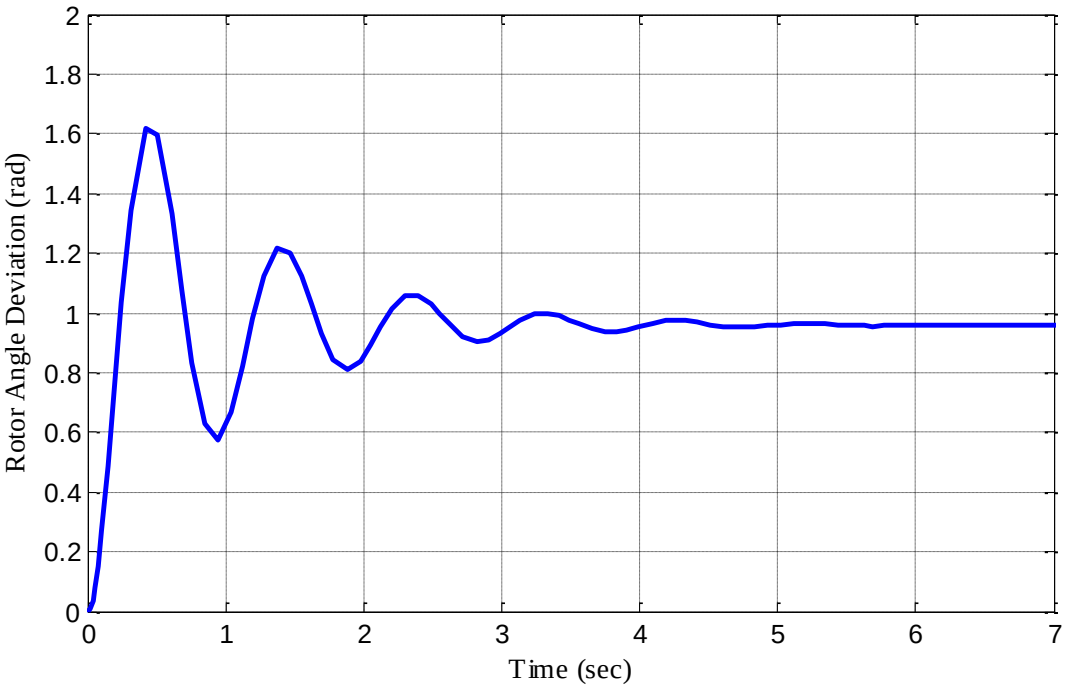

Figure 5.7: Variation of angular position with CPSS (P = 0.9)

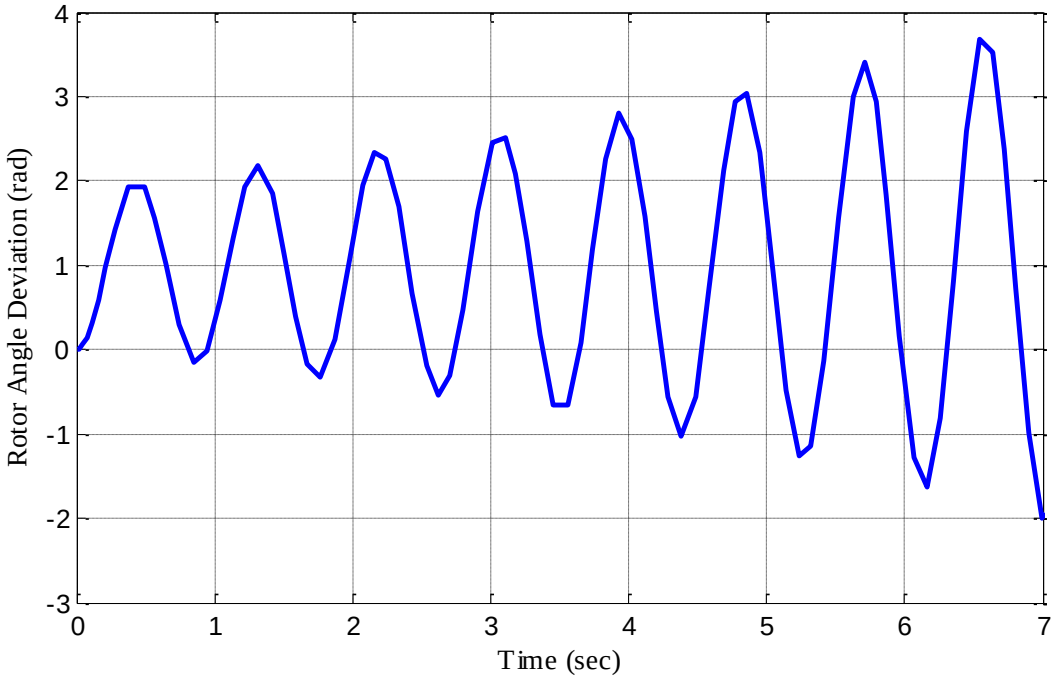

Figure 5.8(a): Variation of angular position with CPSS ($K_{STAB} = 2$)

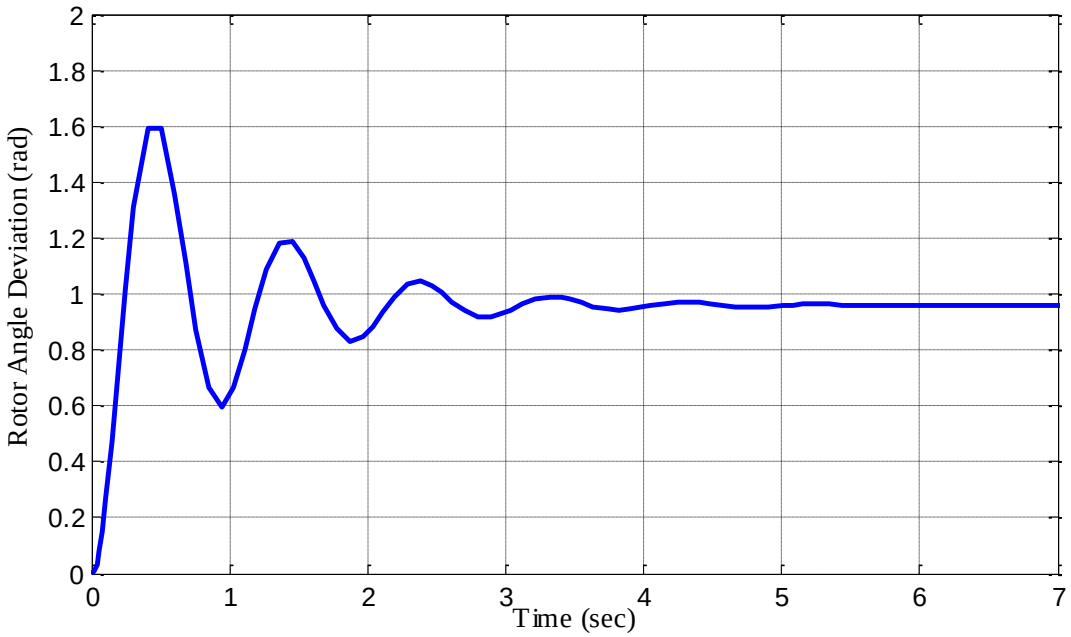

Figure 5.8(b): Variation of angular position with CPSS ($K_{STAB} = 10$)

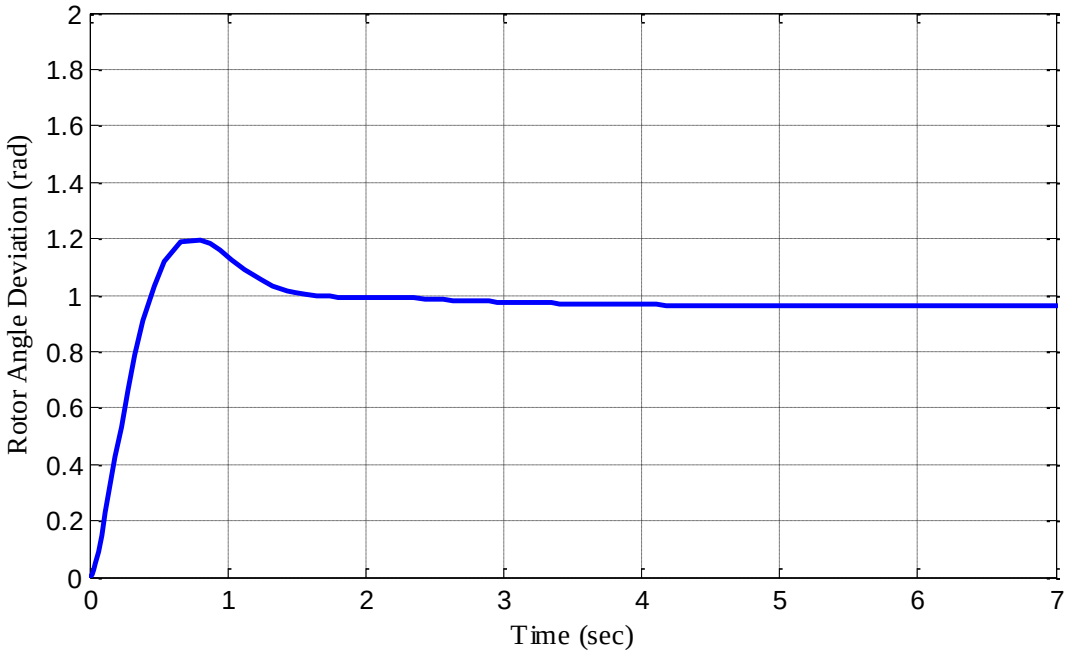

Figure 5.8(c): Variation of angular position with CPSS (K_{STAB} = 40)

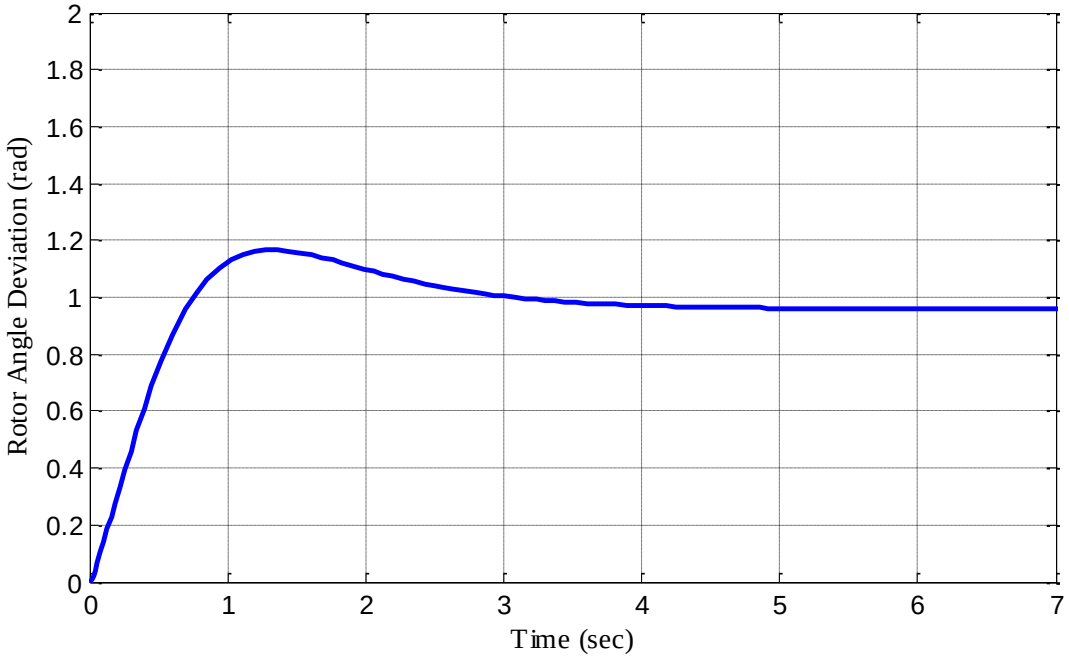

Figure 5.8(d): Variation of angular position with CPSS (K_{STAB} = 80)

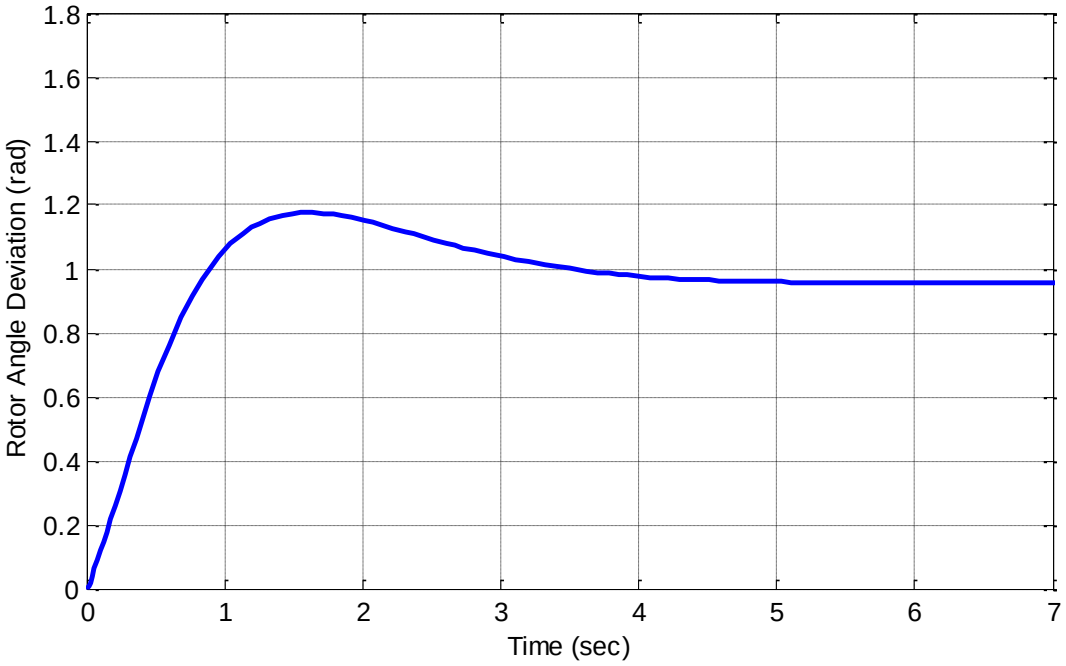

Figure 5.8(e): Variation of angular position with CPSS (K_{STAB} = 100)

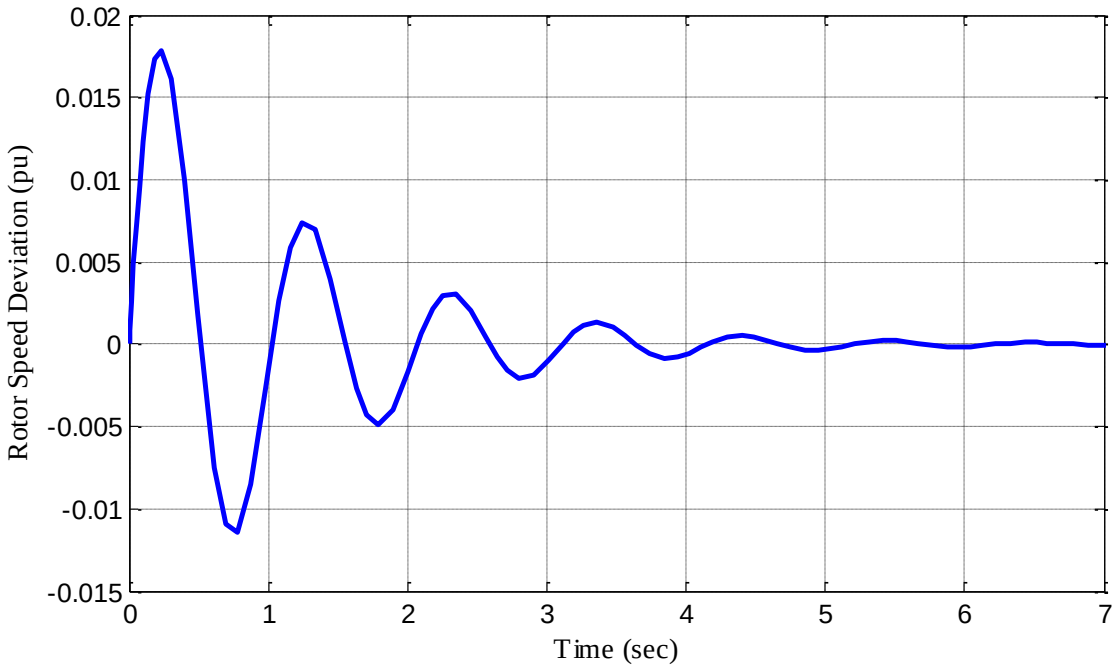

Figure 5.9: Variation of angular speed with CPSS for positive K_5 (P = 0.4)

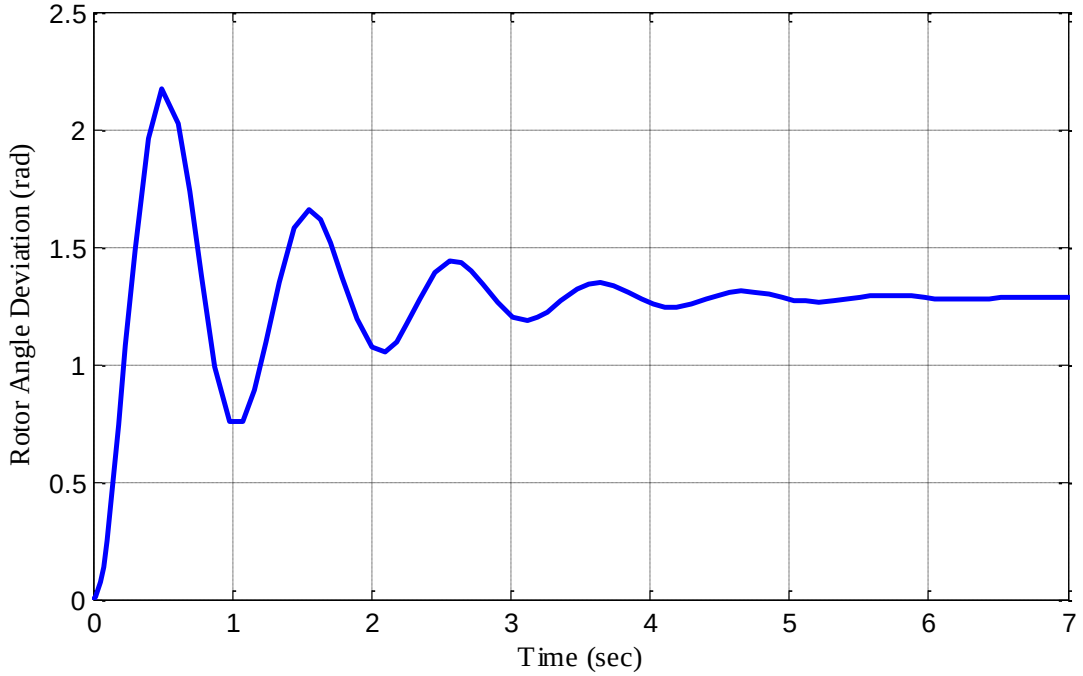

Figure 5.10: Variation of angular position with CPSS for positive K_5 (P = 0.4)

5.5: Result with Fuzzy Logic Based PSS

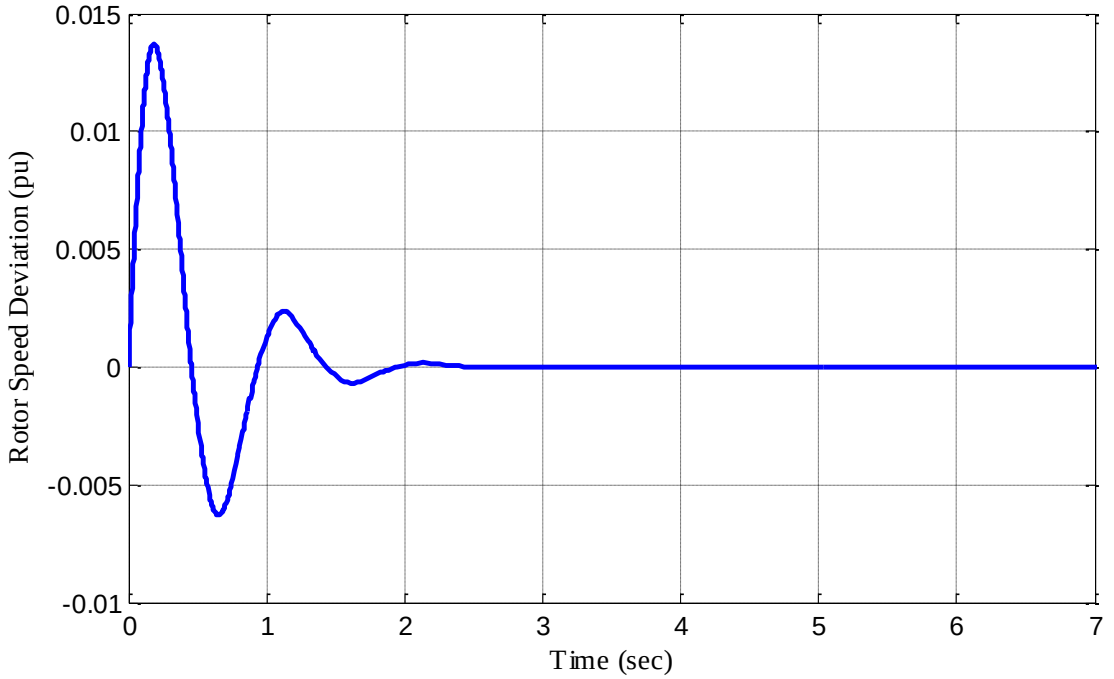

Figure 5.11: Variation of angular speed with FPSS

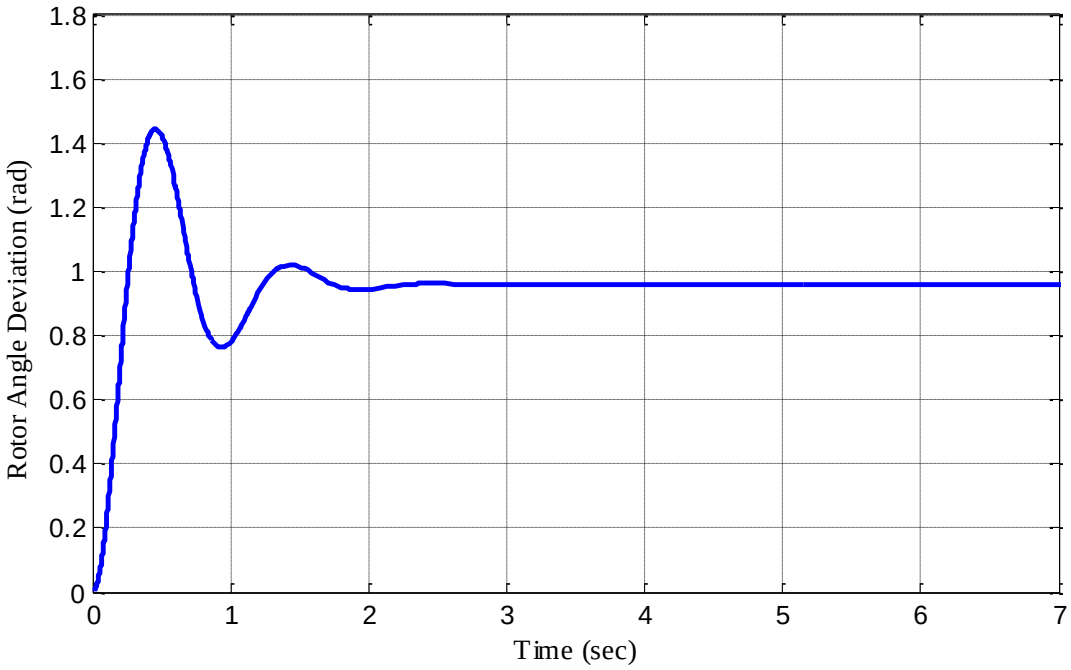

Figure 5.12: Variation of angular position with FPSS

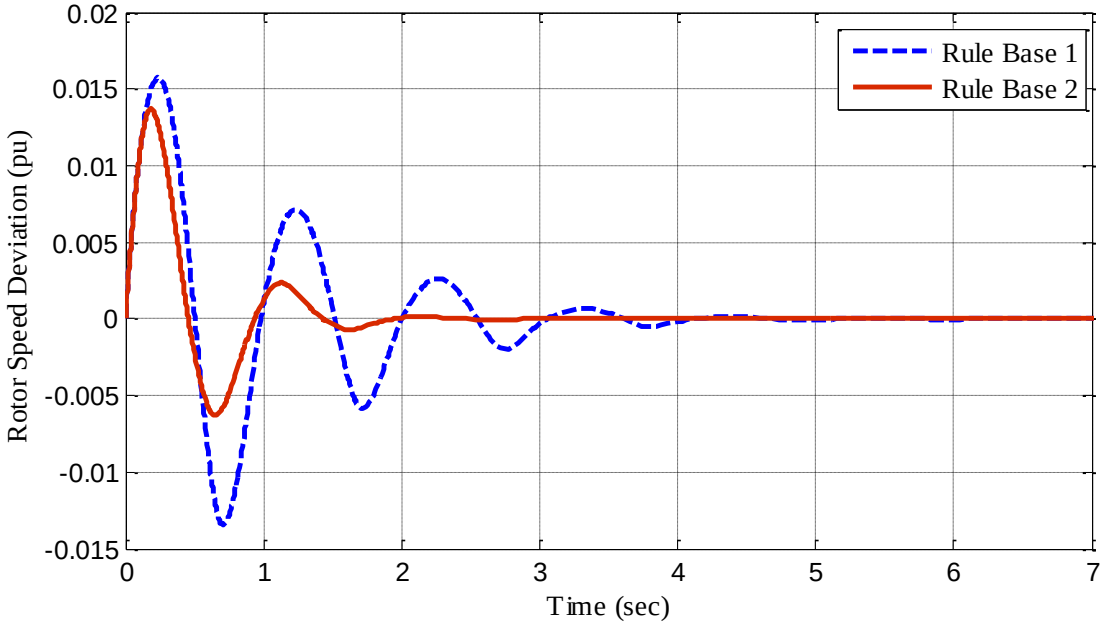

Figure 5.13: Comparison in variation of angular speed between two different fuzzy rule bases

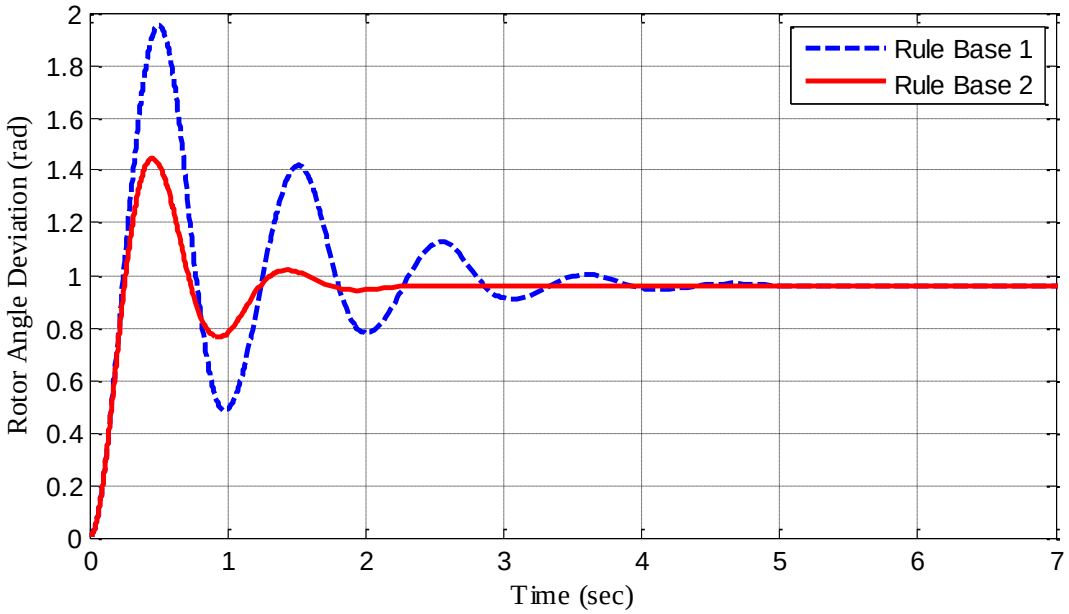

Figure 5.14: Comparison in variation of angular position between two different fuzzy rule bases

5.6 Conventional Vs. Fuzzy Logic Based PSS

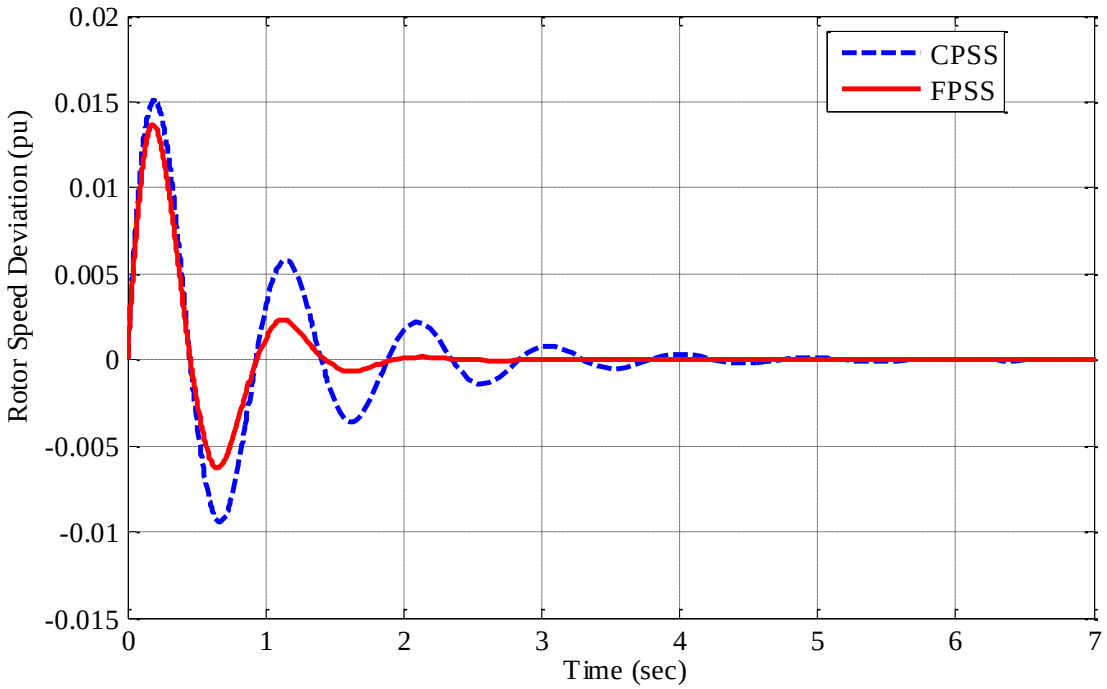

Figure 5.15: Comparison in variation of angular speed with CPSS & FLPSS

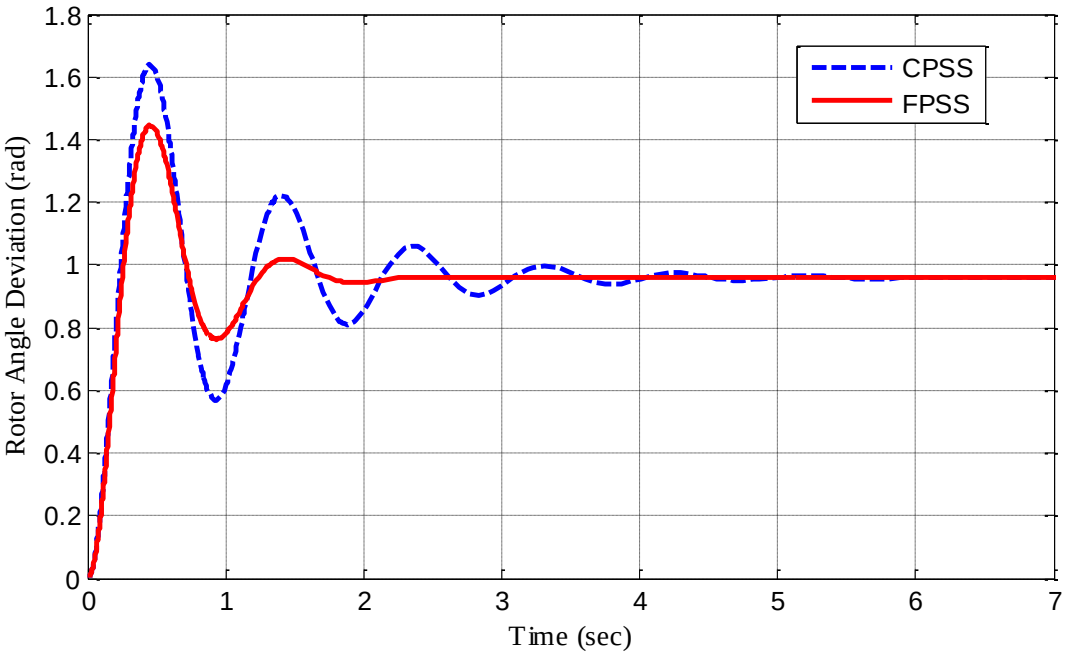

Figure 5.16: Comparison in variation of angular position with CPSS and FLPSS

- Figure 5.2 and Figure 5.3 show the variation of angular speed and angular position of the rotor respectively without AVR.

- Figure 5.4 and Figure 5.5 show the variation of angular speed and angular position of the rotor respectively with AVR only.

- Figure 5.6 and Figure 5.7 show the variation of angular speed and angular position of the rotor respectively with conventional PSS.

- Figures 5.8(a) to 5.8(e) show the variation of angular position of the rotor with conventional PSS at different values of stabilizer gains (K_{STAB}). The responses are better for higher values of stabilizer gain.

- Figure 5.9 and Figure 5.10 show the variation of angular speed and angular position of the rotor respectively with conventional PSS for positive value of K_5 (P = 0.4). For operating condition P > 0.4 the value K5 will be negative, which is normally a practical case.

- Figure 5.11 and Figure 5.12 show the variation of angular speed and angular position of the rotor respectively with Fuzzy based PSS.

- Figure 5.13 and Figure 5.14 show the comparison in variation of angular speed and angular position respectively for two different fuzzy rule bases.

- As shown in Figure 5.15 with fuzzy logic based PSS (FLPSS), the variation in angular position reduces to zero in 2 seconds but with conventional PSS (CPSS), it takes more than 5 seconds to reach to the final steady state value. The oscillations are less pronounced in FLPSS compared to CPSS.

- As shown in Figure 5.16 with fuzzy logic based PSS (FLPSS), the variation in angular speed reduces to zero in 2 seconds but with conventional PSS (CPSS), it takes more than 5 seconds to reach to the final steady state value. The oscillations are less pronounced in FPSS compared to CPSS.

CHAPTER- 6

CONCLUSION AND SCOPE FOR FURTHER WORK

6.1 Conclusion

In this thesis work initially the effectiveness of power system stabilizer in damping power system stabilizer is reviewed. Then the fuzzy logic based power system stabilizer is introduced by taking speed deviation and acceleration of synchronous generator as the input signals to the fuzzy controller and voltage as the output signal. FLPSS shows the better control performance than power system stabilizer in terms of settling time and damping effect. Therefore, it can be concluded that the performance of FLPSS is better than conventional PSS.

6.2 Scope for future work

Having gone through the study of fuzzy logic based PSS (FLPSS) for single machine infinite bus system, the scope of the work is

1. The fuzzy logic based PSS (FLPSS) can be extended to multi machine interconnected system having non-linear industrial loads which may introduce phase shift.

2. The fuzzy logic based PSS with frequency as input parameter can be investigated because the frequency is highly sensitive in weak system, which may offset the controller action on the electrical torque of the machine.

3. Testing using more complex network models can be carried out.

REFERENCES

[1] A. Dysko, W. Leithead, and J. O'Reilly, "Enhanced power system stability by coordinated pss design" , *Power Systems, IEEE Transactions on*, vol. 25, no. 1, pp. 413-422, Feb. 2010.

[2] G. Guralla, R. Padhi and I. Sen , "Power system stabilizers design for interconnected power systems", Power *Systems, IEEE Transactions on*, vol. 25, no. 2, pp. 1042 - 1051,May 2010.

[3] A. Chatterjee, S. Ghoshal, and V. Mukherjee, "A comparative study of single input and dual input power system stabilizer by hybrid evolutionary programming", *in Nature Biologically Inspired Computing, 2009. NaBIC 2009. World Congress on*, Dec. 2009, pp.1047 -1052.

[4] J. Van Ness, F. Brasch, G. Landgren, and S. Naumann, "Analytical investigation of dynamic instability occurring at powerton station", *Power Apparatus and Systems, IEEE Transactions on*, vol. PAS-99, no. 4, pp. 1386 -1395, July 1980.

[5] F. Demello and C. Concordia, "Concepts of synchronous machine stability as affected by excitation control", *Power Apparatus and Systems, IEEE Transactions on*, vol. PAS-88,no. 4, pp. 316 -329, April 1969.

[6] R. Gupta, B. Bandyopadhyay, and A. Kulkarni, "Design of power system stabiliser for single-machine system using robust periodic output feedback controller", *Generation, Transmission and Distribution, IEE Proceedings*-, vol. 150, no. 2, pp. 211 - 216, March 2003.

[7] G. Gurrala and I. Sen, "A modfied heffron-phillip's model for the design of power system stabiliz- ers", *in Power System Technology and IEEE Power India Conference, 2008.POWERCON 2008. Joint International Conference on*, Oct. 2008, pp.1-6.

[8] F. M. H. M. Saidy, "Performance improvement of a conventional power system stabilizer", *International Journal of Electrical Power and Energy Systems*, vol. 150, no.5, pp. 313-323, Oct. 2005.

[9] E. Larsen and D. Swann, "Applying power system stabilizers part i, ii, iii: Practical considerations", *Power Apparatus and Systems, IEEE Transactions on*, vol. PAS-100, no.6, pp. 3034 -3046, June 1981.

[10] T. L. De Mello F.P., P.J. Nolan and J. Undrill, "coordinated application of stabilizers in multi machine power system", *Proceedings of the Twenty-First Annual North-American Power Symposium*, vol. Issue, 9-10, pp. 175 - 184., July 1980.

[11] C. Vournas and J. Mantzaris," Application of qss modeling to stabilizer design for interarea oscillations", *Power Systems, IEEE Transactions on*, vol. 25, no. 4, pp.1910-1917, nov. 2010.

[12] Y. Sudou, A. Takeuchi, and M. Andou, "Development of a Parallel PSS for Inter-area mode power oscillation damping", *0-7803-5569-5/99 © 1999 IEEE.*

[13] P. Kundur, M. Klein, GJ Rogers and M. S. Zywno, "Application of power system stabilizer for enhancement of overall system stability", *IEEE Transactions on Power Systems*,Vol.4,2, May 1989.

[14] M. Klein and P. Kundur,"Analytical investigation of factors influencing power system stabilizers performance", *IEEE transactions on Energy Conversion*, Vol. 7, No. 3, September 1992.

[15] Ziad M. M. Ali and A. I. Malikov," Robust Techniques for Designing Power System Stabilizer", *Journal of Theoretical and Applied Information Technology © 2005-2009 JATIT.*

[16] Joe H. Chow, G.E. Boukarim and A. Murdoch, "Power System Stabilizers as undergraduate Control Design Projects", *IEEE Transaction on Power System*, Vol.19,No. 1, Feb 2004.

[17] P. Kundur, "Effective use of Power System Stabilizers for Enhancement of power system Reliability", *Panel session on system reliability as affected by power System Stabilizers*,1999 IEEE Summer meeting.

[18] Y. Lin, "Systematic approach for the design of a fuzzy power system stabilizer", *in Power System Technology, 2004. PowerCon 2004. 2004 International Conference on*,vol. 1, nov. 2004, pp. 747 - 752 Vol.1.

[19] A. Roosta, H. Khorsand, and M. Nayeripour, "Design and analysis of fuzzy power system stabilizer", *in Innovative Smart Grid Technologies Conference Europe (ISGT Europe),2010 IEEE PES*, Oct. 2010, pp. 1-7.

[20] M.L. Kothari and T.J. Kumar, "A new approach for designing fuzzy logic power system stabilizer", *in Power Engineering Conference, 2007. IPEC 2007. International*, dec.2007, pp. 419 -424.

[21] T. Hussein, M. Saad, A. Elshafei, and A. Bahgat, "Damping inter-area modes ofoscillation using an adaptive fuzzy power system stabilize", *in Control and Automation,2008 16th Mediterranean Conference on*, June 2008, pp. 368 -373.

[22] S. K. Yee and J. Milanovic, "Fuzzy logic controller for decentralized stabilization of multimachine power systems", *Fuzzy Systems, IEEE Transactions on*, vol. 16, no. 4, pp.971 -981, Aug. 2008.

[23] N. Gupta and S.K. Jain, "Comparative analysis of fuzzy power system stabilizer using different membership functions", *International Journal of Computer and Electrical Engineering*, vol. 2, no. 2, April 2010.

[24] M. Ramirez-Gonzalez and O.P.Malik, "Simplifed fuzzy logic controller and its application as a power system stabilizer", *in Intelligent System Applications to Power Systems, 2009.ISAP '09. 15th Interna- tional Conference on*, Nov. 2009, pp. 1-6.

[25] D. Sumina, N. Bulic, and G. Erceg, "Simulation model of neural network based synchronous generator excitation control", *in Power Electronics and Motion Control Conference, 2008. EPE-PEMC 2008*. 13th, Sept. 2008, pp. 556-560.

[26] H. Behbehani, J. Bialek, and Z. Lubosny, "Enhancement of power system stability using fuzzy logic based supervisory power system stabilizer", *in Power and Energy Conference, 2008. PECon 2008. IEEE 2nd International*, Dec. 2008, pp. 479 - 484.

[27] N. Nallathambi and P. Neelakantan, "Fuzzy logic based power system stabilizer", *in E-Tech 2004*, July 2004, pp. 68 - 73.

[28] A. Singh and I. Sen, "A novel fuzzy logic based power system stabilizer for a multimachine system", *in TENCON 2003. Conference on Convergent Technologies for Asia-Paci¯c Region*, vol. 3, Oct. 2003, pp. 1002 - 1006 Vol.3.

[29] H. Toliyat, J. Sadeh, and R. Ghazi, "Design of augmented fuzzy logic power system stabilizers to enhance power systems stability", *Energy Conversion, IEEE Transactions on*, vol. 11, no. 1, pp. 97 -103, Mar 1996.

[30] T. Abdelazim and O. Malik, "An adaptive power system stabilizer using on-line self-learning fuzzy systems", *in Power Engineering Society General Meeting, 2003*, IEEE,vol. 3, July 2003, pp. 1715 - 1720 Vol.

[31] N. I. Voropai and P. V. Etingov, "Application of Fuzzy logic Power system Stabilizers to Transient Stability Improvement in a Large Electric Power System", *0-7803-7459-2/02©2002 IEEE.*

[32] P. Hoang and K. Tomsovic,"Design and analysis of an adaptive fuzzy logic power system stabilizer", *IEEE Transaction on Energy conversion*, Vol.11,No.2, June1996.

[33] Hamid A. Toliyat, j sadeh and Reza Ghazi," Design of augmented fuzzy logic power system stabilizers to enhance power system stability", *IEEE Transaction on Energy Conversion*, Vol.1, No. 1, March 1996.

[34] M. A. M. Hassan and O. P. Malik, "Implementation and laboratory test results for a fuzzylogic based self tuned power system stsbilizer", *IEEE Transaction on Energy Conversion*,Vol.8, No.2, June 1993.

[35] R Ramya and K Selvi," A simple fuzzy excitation control system for synchronous generator*", proceeding of ICETECT 2011 IEEE.*

[36] K. C. Rout and P.C. Panda," An adaptive fuzzy logic based power system stabilizer for enhancement of power system stability", *2010 International Conference on Industrial Electronics, Control and Robotics.*

[37] D.K.Sambariya and R Prasad, "Robust Power System Stabilizer design for single machine infinite bus system with different membership functions for fuzzy logic controller",*978-1-4673-4603-0/12/2012 IEEE.*

[38] D. Murali and M. Rajaram," Damping improvement by fuzzy based power system stabilizers applied in multi-machine power systems", *European Journal of Scientific research*, ISSN 1450- 216X Vol.55 No. 4(2011)pp.506-516.

[39] P. Kundur, J. Paserba, V. Ajjarapu, G. Andersson, A. Bose, C. Canizares, N.Hatziargyriou, D. Hill, A. Stankovic, C. Taylor, T. Van Cutsem, and V. Vittal,"Definition and Classification of Power System Stability" , *IEEE Trans. Power Syst.*, vol.19, no. 2, pp. 1387–1401, May 2004.

[40] P. Kundur, "Power System Stability and Control, McGraw-Hill, 1994.

Appendix-'A'

System Data

A thermal generating station consisting of four 555 MVA, 24 kV, 60 Hz units has been considered as a system. Figure 1 show the system representation. All the network reactances shown in Fig.1 are in pu on 2200MVA, 24 kV base. All the resistances are neglected.

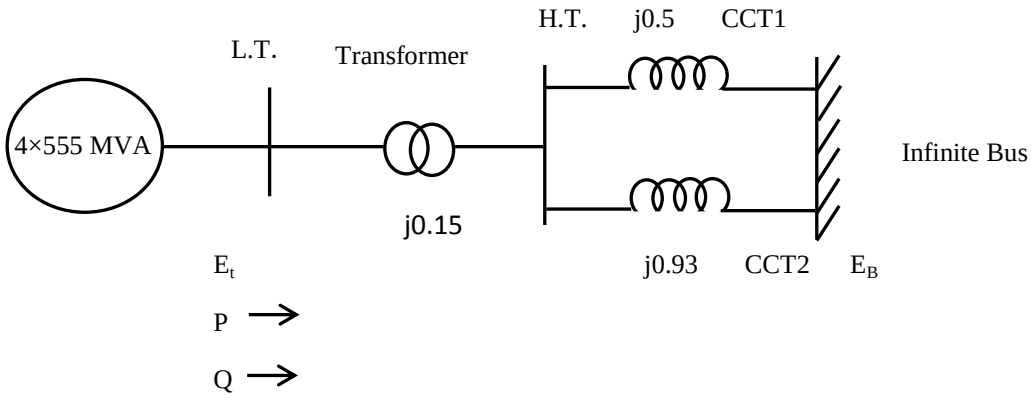

Figure 1: System Representation

Transmission line 2 (CCT2) is isolated by tripping CBs at both ends. The small signal stability characteristics of the above system following the loss of line 2 are considered. The plant output in per unit on 2220 MVA and 24 kV base is as follows:

P = 0.9 , Q = 0.3, Et = 1.0 ∠36°,

Other parameters of the synchronous machine, excitation system and PSS used for modeling the system are as follows:

[a] **Synchronous machine constants:**

X_d = 1.81 pu X_q = 1.76 pu

X'_d = 0.3 pu R_e = 0.003

X_e = 0.65 H = 3.5

f = 60 Hz

[b] **Excitation system constants:**

K_A = 200.0 T_A = 0.05 T_R = 0.015

E_FMAX = 5.0 E_FMIN = ─ 5.0

[c] **PSS Constants:**

K_{STAB} = 9.5 Tw = 1.4 sec

T_1 = 0.154 sec T_2 = 0.033 sec

$V_S(MAX)$ = 0.2 $V_S(MIN)$ = ─ 0.2

Based on the above data the calculated values of K constants are:

K_1 = 0.7643 K_2 = 0.8649 K_3 = 0.3230

K_4 = 1.4187 K_5 = ─ 0.1463 K_6 = 0.4168